Inorg. Chem. **2007**, *46*, 11416–11430

Fe^{III} Complexes of 1,4,8,11-Tetraaza[14]annulenes as Catalase Mimics

Reiner Sustmann,*,‡ Hans-Gert Korth,‡ Diana Kobus,‡ Jörg Baute,‡ Karl-Heinz Seiffert,‡ Elisabeth Verheggen,‡ Eckhard Bill,§ Michael Kirsch,# and Herbert de Groot*,#

Institut für Organische Chemie, Universität Duisburg-Essen, 45117 Essen, Germany, Max-Planck Institut für Bioanorganische Chemie, 45470 Mülheim an der Ruhr, Germany, and Institut für Physiologische Chemie, Universitätsklinikum Essen, 45122 Essen, Germany

Received May 18, 2007

The development of enzyme mimics of catalase which decompose hydrogen peroxide to water and molecular oxygen according to the 2:1 stoichiometry of native catalase and in aqueous solution at pH 7 and at micromolar concentrations of the enzyme model and hydrogen peroxide is reported. For this purpose, iron(III) complexes of 1,4,8,11-tetraaza[14]annulenes are prepared by various procedures. Efficacious preparations utilize reaction of the $[N_4]$ macrocyles with Fe^{II} salts in the presence of triphenylamine, followed by gentle oxidation of the Fe^{II} complexes by molecular oxygen or by tris(4-bromophenyl)aminium hexachloroantimonate. The complexes are characterized by SQUID magnetometry and by Mössbauer, EPR, and UV/vis spectrometry. In the solid state, the iron(III) center of the catalytically active complexes exists in the intermediate (quartet, $S = {}^3/_2$) spin state. Several of these complexes decompose hydrogen peroxide in aqueous buffer solution at pH 7.2 at room temperature with turnover numbers between 40 and 80. The apparent second-order rate constant for hydrogen peroxide decomposition is in the range of 1400–2400 $M^{-1}s^{-1}$, about 3 orders of magnitude lower than the value for native catalase. Besides oxygen production, a non-oxygen releasing pathway of hydrogen peroxide decomposition is unveiled.

Introduction

The catalase enzymes regulate the intracellular level of hydrogen peroxide in living systems by converting two molecules of hydrogen peroxide to two molecules of water and one molecule of oxygen, eq 1.

$$2H_2O_2 \rightarrow 2H_2O + O_2 \qquad (1)$$

The name catalase was coined in 1901 by Loew.[1] The active center of catalases from eucaryotic cells is an iron(III)-protoporphyrin-IX complex; a few manganese(II)-based catalases have been found in procaryotic cells.[2] Numerous investigations have been carried out pursuing different aspects of the enzyme's structures and functions. Several X-ray structures of various iron catalases have been published, providing detailed insight in the location of the Fe-porphyrin system in the enzyme and its protein surroundings.[3−10] Discussions of the present status of the catalytic mechanism of hydrogen peroxide decomposition can be found in refs 11−13.

Numerous attempts have been made to develop synthetic catalase mimics. The majority of such studies were carried out on iron-porphyrin complexes, demonstrating the capability to decompose hydrogen peroxide catalytically. In most cases, however, experiments had to be performed in non-aqueous solvents and/or exhibited low catalytic turnovers.[14,15] In some cases, manganese porphyrins showed a similar

* To whom correspondence should be addressed. Fax: (49)201-183-4259 (R.S.); (49)201-723-5943 (H.d.G.). E-mail: reiner.sustmann@uni-duisburg-essen.de (R.S.); H.de.Groot@uni-duisburg-essen.de (H.d.G.).

‡ Universität Duisburg-Essen.

§ Max-Planck Institut Mülheim an der Ruhr.

Universitätsklinikum Essen.

(1) (a) Loew, O. *Rep. Dep. Agric. Washington* **1901**, *68* (U.S. Department of Agriculture Report Number 68 (1901), 48pp). (b) Loew, O. *Science* **1900**, *11*, 701−702.

(2) Zamocky, M.; Koller, F. *Prog. Biophys. Mol. Biol.* **1999**, *72*, 19−66.

(3) Jouve, H. M.; Gouet, P.; Boudjada, N.; Buisson. G.; Kahn, R.; Duee, E. *J. Mol. Biol.* **1991**, *221*, 1075−1077.

(4) Mate, M. J.; Zamocky, M.; Nykyri, L. M.; Herzog, C.; Alzari, P. M.; Betzel, C.; Koller, F.; Fita, I. *J. Mol. Biol.* **1999**, *286*, 135−149.

(5) Ko, T. P.; Day, J.; Malkin, A. J.; McPherson, A. *Acta Crystallogr., Sect D* **1999**, *55*, 1383−1394.

(6) Putnam, C. D.; Arvai, A. S.; Bourne, Y. *J. Mol. Biol.* **2000**, *296*, 295−309.

(7) Melik-Adamyan, W. R.; Bravo, J.; Carpena, X.; Switala, J.; Mate, M. J.; Fita, I.; Loewen, P. C. *Proteins: Struct., Funct., Genet.* **2001**, *44*, 270−281.

10.1021/ic700961b CCC: $37.00
Published on Web 11/15/2007

reactivity.[16,17] Only a limited number of non-heme iron complexes have been prepared and tested for their catalase-like activity.[18,19] So far, the most active non-heme metal complexes are manganese-salen systems, which are intended for therapeutic purposes.[20,21]

Our interest in Fe^{III} complexes of macrocyclic tetraaza ($[N_4]$) ligands as possible catalase mimics was triggered by recent (and steadily increasing) biological studies on cell damage by "iron".[22−27] Increased levels of H_2O_2 and derived "reactive oxygen species" (ROS) and their interaction with redox-active iron ions have been related to a variety of pathophysiological events, for instance, ischemia-reperfusion related injuries such as heart attack, stroke, and organ dysfunction as well as neurodegenerative disorders such as Alzheimer's, Parkinson's, and Huntington's diseases.[28−33] In particular, the combination of Fe^{II} and hydrogen peroxide, which produces free $HO^{\bullet}$ radicals via the Fenton or Haber−Weiss process,[34,35] is noxious to living organisms. Our investigations are aimed at the development of catalase mimics which should function under conditions as close as possible to physiological situations, in particular, in aqueous solution at pH 7 and at micromolar concentrations of the enzyme model and hydrogen peroxide and also obeying the stoichiometry of native catalase (eq 1). If this turns out to be possible, such mimics might be used in biological applications to protect cells against damage by hydrogen peroxide. A more ambitious goal is the application of the parent ligands to the living systems. Inside cells these ligands are expected to form the corresponding Fe^{III} complexes with the iron ions of the so-called "labile iron pool", thus becoming "in situ" catalase mimics which might regulate the concentration of free redox-active iron ions and the concentration of hydrogen peroxide at the same time.

Our studies are based on Fe^{III} complexes first reported by Melnyk et al.,[18] who describe their complexes as "catalase mimics". However, with regard to the reaction conditions required for H_2O_2 decomposition, we demonstrated that the complexes of Melnyk et al. cannot reasonably be considered as true catalase mimics.[36] Therefore, the iron complexes described in the present contribution were designed according to the mechanism by which native catalase decomposes hydrogen peroxide.[2,12,13,37] In the catalase cycle, the iron(III) center of the enzyme's resting state is oxidized by a first molecule of H_2O_2 to "Compound I",[38,39] a highly reactive iron(IV)oxo (ferryl-oxo)-porphyrin radical cation intermediate, and H_2O_2 is reduced to water. Compound I is subsequently reduced back to the resting state by a second H_2O_2 molecule, and molecular oxygen and the second molecule of water are released. In general, an enzyme model compound does not need to follow the same mechanism as the biological system. However, with regard to the fact that eq 1 refers to a disproportionation process, two molecules of H_2O_2 need to react with the species involved in the catalytic cycle: one H_2O_2 acting as an oxidant, the other H_2O_2 acting as a reductant. Any other (non-multiple) overall stoichiometry of H_2O_2 decomposition would require the oxidation or reduction of an auxiliary substrate, which might even be a ligand of the complex. In our opinion, metal complexes which degrade H_2O_2 without obeying eq 1 thus should not be considered as "catalase mimics". Conclusively, the highest chance for developing a functional catalase mimic, which would not involve conversion of a third substrate, is to facilitate the formation of an intermediate that is or acts similar to Compound I. In recent years, several heme and non-heme ferryl-oxo species (Fe^{IV}═O) have been generated and characterized.[40−44] In order to further allow formation of a π-radical cation, the ligand should possess a high

(8) Murshudov, G. N.; Grebenko, A. I.; Brannigan, J. A.; Antson, A. A.; Barynin, V. V.; Dodson, E. J.; Dauter, Z.; Wilson, K. S.; Melik-Adamyan, W. R. *Acta Crystallogr., Sect D* **2002**, *58*, 1972−1982.
(9) Carpena, X.; Soriano, M.; Klotz, M. G.; Duckworth, H. W.; Donald, L. J.; Melik-Adamyan, W. R.; Fita, I.; Loewen, P. C. *Proteins: Struct., Funct., Genet.* **2003**, *50*, 423−436.
(10) Carpena, X.; Loprasert, S.; Mongkolsuk, S.; Switala, J.; Loewen, P. C.; Fita, I. *J. Mol. Biol.* **2003**, *327*, 475−489.
(11) Kirkman, H. N. M.; Rolfo; A. M.; Ferraris; Gaetani, G. F. *J. Biol. Chem.* **1999**, *274*, 13908−13914.
(12) Nicholls, P.; Fita, I.; Loewen, P. C. *Adv. Inorg. Chem.* **2001**, *51*, 51−106.
(13) Kirkman, H. N.; Gaetani, G. F. *Trends Biochem. Sci.* **2007**, *32*, 44−50.
(14) Traylor, T. G. *Acc. Chem. Res.* **1981**, *14*, 102−109.
(15) Robert, A.; Loock, B.; Momenteau, M.; Meunier, B. *Inorg. Chem.* **1991**, *30*, 706−711.
(16) Balasubramanian, P. N.; Schmidt, E. S.; Bruice, T. C. *J. Am. Chem. Soc.* **1987**, *109*, 7865−7873.
(17) Day, B. J.; Fridovich, I.; Crapo, J. D. *Arch. Biochem. Biophys.* **1997**, *347*, 256−262.
(18) Melnyk, A. C.; Kildahl, N. K.; Rendina, A. R.; Busch, D. H. *J. Am. Chem. Soc.* **1979**, *101*, 3232−3240.
(19) Cairns, C. J.; Heckman, R. A.; Melnyk, A. C.; Davis, W. M.; Busch, D. H. *J. Chem. Soc., Dalton Trans.* **1987**, 2505−2510.
(20) Doctrow, S.; Huffman, K.; Marcus, C. B.; Musleh, W.; Buce, A.; Baudry, M.; Malfroy, B. *Adv. Pharmacol.* **1997**, *38*, 247−269.
(21) Doctrow, S. R.; Huffman, K.; Marcus, C. B.; Tocco, G.; Malfroy, E.; Adinolfi, C. A.; Kruk, H.; Baker, K.; Lazarowych, N.; Mascarenhas, J.; Malfroy, B. *J. Med. Chem.* **2002**, *45*, 4549−4558.
(22) Halliwell, B.; Gutteridge, J. M. C. *Methods Enzymol.* **1990**, *186*, 1−85.
(23) Halliwell, B.; Gutteridge, J. M. C. *Free Radicals in Biology and Medicine*, 3rd ed.; Oxford University Press, Inc.: New York, 1999.
(24) Kakhlon, O.; Cabantchik, Z. I. *Free Radical Biol. Med.* **2002**, *33*, 1037−1046.
(25) Rauen, U.; Petrat, F.; Li. T.; de Groot, H. *FASEB J.* **2000**, *14*, 1953−1964.
(26) Rauen, U.; Petrat, F.; Sustmann, R.; de Groot, H. *J. Hepatol.* **2004**, *40*, 605−613.
(27) Stäubli, A.; Boelsterli, U. A. *Am. J. Physiol.* **1998**, *274*, G1031−G1037.
(28) Carbonell, T.; Rama, R. *Curr. Med. Chem.* **2007**, *14*, 857−-874.
(29) Crimi, E.; Sica, V.; Slutsky, A. S.; Zhang, H.; Williams-Ignarro, S.; Ignarro, L. J.; Napoli, C. *Free Radical Res.* **2006**, *40*, 665−672.
(30) de Groot, H.; Rauen, U. *Transplant. Proc.* **2007**, *39*, 481−484.
(31) Loh, K. P.; Huang, S. H.; De Silva, R.; Tan, B. K.; Zhu, Y. Z. *Curr. Alzheimer Res.* **2006**, *3*, 327−337.
(32) Margaill, I.; Plotkine, M.; Lerouet, D. *Free Radical Biol. Med.* **2005**, *39*, 429−443.
(33) Zweier, J. L.; Talukder, M. A. *Cardiovasc. Res.* **2006**, *70*, 181−190.
(34) Haber, F.; Weiss, J. *Proc. R. Soc. (London)* **1934**, *147*, 322−351.
(35) Goldstein, S.; Meyerstein, D. *Acc. Chem. Res.* **1999**, *32*, 547−550.
(36) Autzen, S.; Korth, H.-G.; de Groot, H.; Sustmann, R. *Eur. J. Org. Chem.* **2001**, 3119−3125.
(37) Schonbaum, G. R.; Chance, B. In *The Enzymes*; Boyer, P. D., Ed.; Academic Press: New York, 1976; Vol. 13, p 363−408.
(38) Chance, B. *Acta Chem. Scand.* **1947**, *1*, 236−267.
(39) Jones, P.; Dunford, H. B. *J. Inorg. Biochem.* **2005**, *99*, 2292−2298.
(40) Fujii, H. *Coord. Chem. Rev.* **2002**, *226*, 51−60.
(41) Costas, M.; Mehn, M. P.; Jensen, M. P.; Que, L. *Chem. Rev.* **2004**, 939−986.
(42) Krebs, C.; Fujimori, D. G.; Walsh, C. T.; Bollinger, J. M. *Acc. Chem. Res.* **2007**, *40*, 484−492.
(43) Que, L. *Acc. Chem. Res.* **2007**, *40*, 493−500.
(44) Nam, W. *Acc. Chem. Res.* **2007**, *40*, 522−531.

Scheme 1. Ligands and Iron Complexes Prepared in This Study

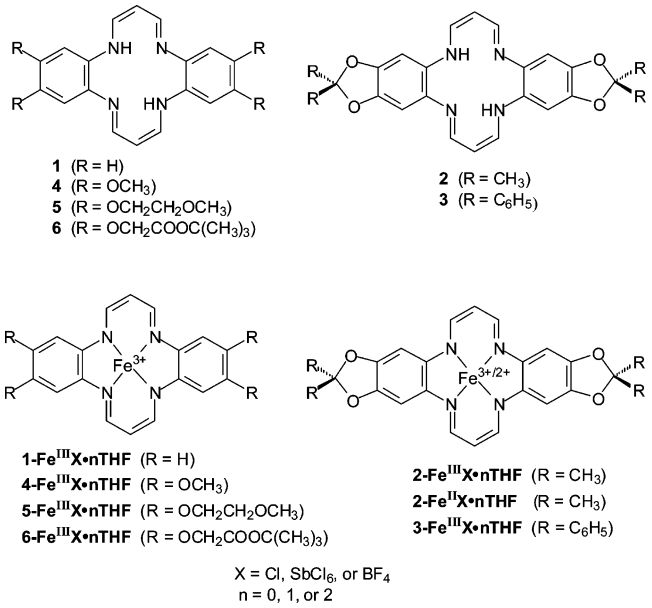

electron density in a cyclic, conjugated π-system. We therefore selected as a starting point 5,14-dihydro-5,9,14,-18-tetraaza-dibenzo[*a*,*h*]cyclotetradecene (**1**, Scheme 1), a ligand which has been known for a long time. An Fe^{II} but not an Fe^{III} complex of this system has been described.[45,46] From the 6,8,15,17-tetramethyl-substituted derivative of **1**, an Fe^{II} and a five-coordinate, high-spin Fe^{III} complex have been prepared and analyzed in terms of structure and reactivity.[46−49] A few other iron complexes of derivatives of **1** have been described,[50,51] but in no case were the Fe^{III} complexes considered as potential catalase mimics, i.e., tested with respect to their reactivity with hydrogen peroxide.

In our studies we equipped the parent 5,14-dihydro-5,9,-14,18-tetraaza-dibenzo[*a*,*h*]cyclotetradecene (**1**) with electron-releasing oxygen substituents in order to increase the electron density of the π-system. In a preliminary communication[52] we presented evidence that the five-coordinate Fe^{III}-tetrafluoroborate complex of ligand **2** (**2-Fe^{III}BF$_4$**) fulfills the condition of producing oxygen from hydrogen peroxide at pH 7 and at micromolar concentrations of both the catalyst and H_2O_2. In a recent biological study we found evidence for our hypothesis of intracellular formation of an iron complex of this ligand.[53] In another study it was shown that **2-Fe^{III}** in fact protects hepatocytes against damage by iron overload.[26]

In the present contribution we report on the synthesis of tetraoxygen-substituted 5,14-dihydro-5,9,14,18-tetraaza-dibenzo[*a*,*h*]cyclotetradecenes (**2**−**6**), the preparation of their Fe^{III} complexes, and the capability of the Fe^{III} complexes to decompose hydrogen peroxide to oxygen and water under conditions which we consider rendering them as true catalase mimics. For comparison, the reactivity of the Fe^{III} complex of the parent ligand **1** toward hydrogen peroxide will also be described. A number of theroretical studies have shown that the spin state of the reactive iron species, especially that of the compound I intermediates, plays a pivotal role for the mechanisms of heme enzymes like the P450 cytochromes or catalases.[54−56] The resting state of native catalase is characterized by Fe^{III}-porphyrin in the high-spin (sextet, $S = {}^5/_2$) state.[57−59] The metal ion is pentacoordinate, with the porphyrin ligand being attached to the protein by proximal coordination to a tyrosylate anion, leaving the distal position for hydrogen peroxide association. Low-spin (doublet, $S = {}^1/_2$) iron(III) complexes of heme derivatives display the metal ion hexacoordinate. The reactive intermediate compound I is theoretically predicted to exist in nearly degenerate doublet or quartet states.[54−56]

Therefore, the spin state of the Fe^{III} complexes in the present study is established by Mössbauer spectrometry and SQUID magnetometry, revealing that in the solid state the iron(III) center of the catalytically active complexes resides in the intermediate (quartet, $S = {}^3/_2$) spin state. In a recent theoretical study,[60] we found evidence that in the aqueous solution the hydrogen peroxide decomposition may proceed from the low-spin ($S = {}^1/_2$) as well as from the intermediate-spin state of hexacoordinated Fe^{III} in these complexes, whereas the high-spin ($S = {}^5/_2$) state should be unreactive. This is nicely confirmed by the results reported below.

Experimental Section

Analytical Equipment. ^{1}H and ^{13}C NMR spectra: Bruker DRX 500 and Varian Gemini 200. Melting points (uncorrected): Elektrothermal 9100. IR: Bio-Rad Series FTS 135 FT-IR. UV/vis: Varian Cary 300 Bio. EPR: Bruker ESP 300E. Elemental analysis: Carlo Erba 1010 CHNSO. Magnetic susceptibilities: Quantum Design MPMS2. ESI-TOF: Bruker Daltonic BioTOF III. Oxygen measurements: Hansatech DW1/CB1-D3. Iron analysis: atomic absorption spectrometer Unicam 939.

Synthesis. The following compounds were prepared following published procedures: 2,2-dimethyl-benzo[1,3]dioxole-4,5-diamine,[61] 2,2-dimethyl-benzo[1,3]dioxole,[62] 1,2-bis-(2-methoxy-

(45) Hiller, H.; Dimroth, P.; Pfitzner, H. *Liebigs Ann. Chem.* **1968**, *717*, 137−147.
(46) Müller, R.; Wöhrle, D. *Makromol. Chem.* **1975**, *176*, 2775−2795.
(47) Goedken, V. L.; Peng, S.-M.; Park, Y. *J. Am. Chem. Soc.* **1974**, *96*, 284−285.
(48) Goedken, V. L.; Park, Y. *J. Chem. Soc., Chem. Commun.* **1975**, 214−215.
(49) Weiss, M. C.; Bursten, B.; Peng, S.-H.; Goedken, V. L. *J. Am. Chem. Soc.* **1976**, *98*, 8021−8031.
(50) Jäger, E. G. *Z. Anorg. Allg. Chem.* **1969**, *364*, 177−191.
(51) Nishida, Y.; Sumita, A.; Ashida, K. H.; Oshima, H.; Kida, S.; Maeda, Y. *J. Coord. Chem.* **1979**, *9*, 161−166.
(52) Paschke, J.; Kirsch, M.; Korth, H.-G.; de Groot, H.; Sustmann, R. *J. Am. Chem. Soc.* **2001**, *123*, 11099−11100.
(53) Rauen, U.; Li, T.; Sustmann, R.; de Groot, H. *Free Radical Biol. Med.* **2004**, *37*, 1369−1383.
(54) Shaik, S.; Kumar, D.; de Visser, S. P.; Altun, A.; Thiel, W. *Chem. Rev.* **2005**, *105*, 2279−2328.
(55) Shaik, S.; Hirao, H.; Kumar, D. *Acc. Chem. Res.* **2007**, *40*. 532−542.
(56) de Visser, S. P. *Inorg. Chem.* **2006**, *45*, 9551−9557.
(57) Chouchane, S.; Lippai, I.; Magliozzo, R. S. *Biochemistry* **2000**, *39*, 9975−9983.
(58) Lukat-Rodgers, G. S.; Wengenack, N. L.; Rusnak, F.; Rodgers, K. R. *Biochemistry* **2000**, *39*, 9984−9993.
(59) Hildebrand, D. P.; Burk, D. L.; Maurus, R.; Ferrer, J. C.; Brayer, G. D.; Mauk, A. G. *Biochemistry* **1995**, *34*, 1997−2005.
(60) Sicking, W.; Korth, H.-G.; Jansen, G.; de Groot, H.; Sustmann, R. *Chem.−Eur. J.* **2007**, *13*, 4230−4245.
(61) Cai, S. X.; Kher, S. M.; Zhou, Z.-L.; Ilyin, V.; Espitia, S. A.; Tran, M.; Hawkinson, R. M.; Woodward, R. M.; Weber, E.; Keana, J. F. W. *J. Med. Chem.* **1997**, *40*, 730−738.
(62) de Sloof, G. *Recl. Trav. Chim. Pays-Bas* **1935**, *54*, 995−1010.

ethoxy)-benzene,[63] 2,2-dimethyl-5-nitro-benzo[1,3]dioxole,[62] 1,2-bis-(2-methoxy-ethoxy)-4-nitro-benzene,[64] 2,2-dimethyl-5,6-dinitro-benzo[1,3]dioxole,[62] 1,2-bis-(2-methoxy-ethoxy)-4,5-dinitro-benzene,[62] 1,2-dihydroxy-4,5-dinitro-benzene,[62] 1,2-dimethoxy-4,5-dinitro-benzene,[62] 1,2-dimethoxy-4,5-diamino-benzene,[65] propinal,[66] 5,14-dihydro-5,9,14,18-tetraaza-dibenzo[*a*,*h*]cyclotetradecene (**1**),[45] 5,14-dihydro-5,9,14,18-tetraaza-dibenzo[*a*,*h*]cyclotetradecene-iron(III) iodide (**1-Fe^{III}I**),[45] and 6,8,15,17-tetramethyl-5,14-dihydro-5,9,14,-18-tetraaza-dibenzo[*a*,*h*]cyclotetradecene.[67]

The preparative procedures for the ligand precursors 1,2-diacetoxy-4,5-dinitro-benzene, 2,2-diphenyl-5,6-dinitro-benzo[1,3]-dioxole, 4,5-bis-(2-methoxy-ethoxy)-benzene-1,2-diamine, 4,5-diacetoxy-benzene-1,2-diamine, 2,2-diphenyl-5,6-diamino-benzo[1,3]dioxole, (2-*tert*-butoxycarbonylmethoxy-4,5-dinitro-phenoxy)-acetic acid *tert*-butyl ester, and (2-*tert*-butoxycarbonylmethoxy-4,5-diamino-phenoxy) acetic acid *tert*-butyl ester are given as Supporting Information.

5,14-Dihydro-5,9,14,18-tetraaza-di(2,2-dimethyl-[5,6]benzo-[1,3]dioxolo)[*a*,*h*]cyclotetradecene (2). A solution of propinal (3.4 g, 62.5 mmol) in ethanol (10 mL) was added dropwise to a stirred solution of 2,2-dimethyl-benzo[1,3]dioxole-4,5-diamine (11.3 g, 62.5 mmol) in ethanol (150 mL). After completion of the addition the mixture was refluxed with stirring for 4 h and cooled to room temperature, and the precipitate was filtered off. The residue was recrystallized from ethanol and dried in vacuum over anhydrous calcium chloride to afford 4.83 g (11.2 mmol, 36%) of the dark brownish-red product. Mp: 274 °C. ^{1}H NMR (500 MHz, $CDCl_3$): δ = 1.62 (s, 12 H, CH_3), 4.77 (t, $^3J_{H,H}$ = 6.3 Hz, 2 H, 7,16-H), 6.38 (s, 4 H, 1,4,10,13-H), 7.26 (dd, $^3J_{H,H}$ = 6.3 Hz, $^4J_{H,H}$ = 6.2 Hz, 4 H, 6,8,15,17-H), 14.07 (t, $^3J_{H,H}$ = 6.3 Hz, 2 H, 5,14-H) ppm. ^{13}C NMR (125 MHz, $CDCl_3$): δ = 25.7 (CH_3), 94.6 (1,4,10,13-C), 95.7 (7,16-C), 118.1 [$C(CH_3)_2$], 131.7 (4a,9a,13a,18a-C), 144.5 (2,3,11,12-C), 144.8 (6,8,15,17-C) ppm. UV/vis ($CHCl_3$): λ_{max} (lg ϵ) = 357 (4.47), 370 (4.47) 453 (4.31), 478 (4.30) nm. Elemental analysis calcd (%) for $C_{24}H_{24}N_4O_4$ (432.48): C, 66.65; H, 5.59; N, 12.96. Found: C, 66.78; H, 5.97; N, 12.96.

5,14-Dihydro-5,9,14,18-tetraaza-di(2,2-diphenyl-[5,6]benzo-[1,3]dioxolo)[*a*,*h*]cyclotetradecene (3). A solution of propinal (1.5 g, 27.7 mmol) in ethanol (1.5 mL) was added rapidly to a stirred slurry of 2,2-diphenyl-5,6-diamino-benzo[1,3]dioxole (8.0 g, 26.3 mmol) in ethanol (450 mL). The mixture was refluxed with stirring for 72 h and cooled to room temperature, and the precipitate was filtered off, washed four times with cold ethanol (10 mL each), and dried in vacuum over anhydrous calcium chloride to afford 3.7 g (5.3 mmol, 41%) of the crystalline brownish-red product. Mp(dec): 90 °C. ^{1}H NMR (500 MHz, $CDCl_3$): δ = 4.77 (t, $^3J_{H,H}$ = 6.3 Hz, 2 H, 7,16-H), 6.51 (s, 4 H, 1,4,10,13-H), 7.25 (dd, $^3J_{H,H}$ = 6.3 Hz, $^4J_{H,H}$ = 6.3 Hz, 4 H, 6,8,15,17-H), 7.53−7.32 (m, 20H, C_6H_5), 14.12 (t, $^3J_{H,H}$ = 6.3 Hz, 2 H, 5,14-H) ppm. ^{13}C NMR (125 MHz, $CDCl_3$): δ = 94.9 (1,4,10,13-C), 95.9 (7,16-C), 117.0 (CPh_2), 126.3 [*m*-C(C_6H_5)], 128.3 [*o*-C(C_6H_5)], 129.1 [*p*-C(C_6H_5)], 132.3 (4a,9a,13a,18a-C), 140.1 [*ipso*-C(C_6H_5)], 144.6 (2,3,11,12-C), 144.7 (6,8,15,17-C) ppm. UV/vis (buffer pH 7.4): λ_{max} (lg ϵ) = 269-(4.24), 358(4.35), 369(4.35), 458(4.24), 479(4.20) nm. Elemental analysis calcd (%) for $C_{44}H_{32}N_4O_4 \cdot H_2O$ (698.78): C, 75.63; H, 4.90; N, 8.02. Found: C, 75.75; H, 4.89; N, 8.25.

2,3,11,12-Tetramethoxy-5,14-dihydro-5,9,14,18-tetraaza-dibenzo[*a*,*h*]cyclotetradecene (4). A solution of propinal (0.5 mL, 8.9 mmol) in dry trichloromethane (10 mL) was added dropwise at 40 °C under argon atmosphere to a stirred solution of 1,2-dimethoxy-4,5-diamino-benzene (1.5 g, 8.9 mmol) in dry trichloromethane (50 mL). After completion of addition, the mixture was refluxed for 4 h, and the formed precipitate was filtered off and washed with *n*-heptane, acetone, and diethyether (5 mL each) to give 0.50 g (1.21mmol, 27%) of the red-brown product. Mp: 308−310 °C. ^{1}H NMR (500 MHz, $CDCl_3$): δ = 3.71 (s, 12 H, CH_3), 4.83 (t, $^3J_{H,H}$ = 6.3 Hz, 2 H, 7,16-H), 6.77 (s, 4 H, 1,4,10,13-H), 7.66 (dd, $^3J_{H,H}$ = 6.2 Hz, $^4J_{H,H}$ = 6.3 Hz, 4 H, 6,8,15,17-H), 14.25 (t, $^3J_{H,H}$ = 6.3 Hz, 2 H, 5,14-H) ppm. ^{13}C NMR (125 MHz, $CDCl_3$): δ = 55.9 (CH_3), 95.4 (7,16-C), 98.6 (1,4,10,13-C), 130.1 (4a,9a,13a,18a-C), 145.9 (6,8,15,17-C), 146.4 (2,3,11,12-C) ppm. UV/vis (DMF): λ_{max} (lg ϵ) = 275 (4.35), 370 (4.75), 439 (4.57), 464 (4.58) nm. Elemental analysis calcd (%) for $C_{22}H_{24}N_4O_4$ (408.45): C, 64.69; H, 5.92; N, 13.72. Found: C, 64.78; H, 5.79; N, 13.88.

2,3,11,12-Tetrakis-(2-methoxy-ethoxy)-5,14-dihydro-5,9,14,-18-tetraaza-dibenzo[*a*,*h*]cyclotetradecene (5). A solution of propinal (2.1 g, 39.0 mmol) in ethanol (15 mL) was added dropwise to a stirred solution of 4,5-bis-(2-methoxy-ethoxy)-benzene-1,2-diamine (10.0 g, 39.0 mmol) in ethanol (200 mL). After completion of addition, the mixture was refluxed with stirring for 5 h and cooled to room temperature, and the precipitate was filtered off and washed with cold THF (20 mL). The residue was recrystallized from ethanol and dried in vacuum over anhydrous calcium chloride to afford 2.55 g (4.36 mmol, 22.4%) of the yellow product. Mp: 215 °C. ^{1}H NMR (500 MHz, $CDCl_3$): δ = 3.42 (s, 12 H, CH_3), 3.69−3.71 (m, 8 H, CH_2OCH_3), 4.85−4.87 (m, 8 H, $CH_2CH_2OCH_3$), 4.86 (t, $^3J_{H,H}$ = 6.3 Hz, 2 H, 7,16-H), 6.60 (s, 4 H, 1,4,10,13-H), 7.39 (dd, $^3J_{H,H}$ = 6.2 Hz, $^4J_{H,H}$ = 6.3 Hz, 4 H, 6,8,15,17-H), 14.21 (t, $^3J_{H,H}$ = 6.3 Hz, 2 H, 5,14-H) ppm. ^{13}C NMR (125 MHz, $CDCl_3$): δ = 59.1 (CH_3), 69.6 (CH_2OCH_3), 71.2 ($CH_2CH_2OCH_3$), 95.9 (7,16-C), 102.1 (1,4,10,13-C), 132.0 (4a,9a,13a,18a-C), 145.1 (6,8,15,-17-C), 146.6 (2,3,11,12-C) ppm. UV/vis (DMF): λ_{max} (lg ϵ) = 273 (4.42), 372 (4.70), 439 (4.52), 463 (4.52) nm. HRMS (EI, 70 eV) calcd for $C_{30}H_{40}N_4O_8$ *m*/*z*: 584.2846 [M^+]. Found: 584.2843.

2,3,11,12-Tetrakis-(acetoxy-*tert*-butylester)-5,14-dihydro-5,9,-14,18-tetraaza-dibenzo[*a*,*h*]cyclotetradecene (6). A solution of propinal (0.3 mL, 5.4 mmol) in dry trichloromethane (10 mL) was added dropwise at 40 °C under argon atmosphere to a stirred solution of (2-*tert*-butoxycarbonylmethoxy-4,5-diamino-phenoxy)-acetic acid *tert*-butyl ester (2.0 g, 5.4 mmol) in dry trichloromethane (50 mL). After completion of addition, the mixture was refluxed for 4 days and the solvent evaporated. The residue was purified by flash chromatography on silica gel (toluene/ethyl acetate 3:1) to afford, after evaporation of the solvent, 0.30 g (0.4 mmol, 28%) of dark green crystals. Mp: 168−169 °C. ^{1}H NMR (500 MHz, $CDCl_3$): δ = 1.45 (s, 36 H, CH_3), 4.51 (s, 8 H, OCH_2CO), 4. 87 (t, $^3J_{H,H}$ = 6.3 Hz, 2 H, 7,16-H), 6.56 (s, 4 H, 1,4,10,13-H), 7.37 (dd, $^3J_{H,H}$ = 6.2 Hz, $^4J_{H,H}$ = 6.3 Hz, 4 H, 6,8,15,17-H), 13.98 (t, $^3J_{H,H}$ = 6.3 Hz, 2 H, 5,14-H) ppm. ^{13}C NMR (125 MHz, $CDCl_3$): δ = 28.1 [$C(CH_3)_3$], 67.8 (CH_2OCH_3), 82.2 [$C(CH_3)_3$], 96.2 (7,-16-C), 102.3 (1,4,10,13-C), 132.4 (4a,9a,13a,18a-C), 145.2 (6,8,-15,17-C), 145.7 (2,3,11,12-C), 168.2 (C=O) ppm. UV/vis (DMF): λ_{max} (lg ϵ) = 278 (4.08), 361 (4.53), 373 (4.58), 437 (4.36), 460 (4.37) nm. Elemental analysis calcd (%) for $C_{42}H_{56}N_4O_{12}$ (808.91): C, 62.36; H, 6.98; N, 6.93. Found: C, 62.55; H, 7.12; N, 6.99.

Preparation of Fe^{III} Complexes. For the preparation of Fe^{III} complexes of ligands **1**−**6** various procedures were attempted,

(63) Budesinsky, Z. A. V. *Coll. Czech. Chem. Commun.* **1971**, *36*, 2527−2539.
(64) Page, D. F.; Clinton, R. O. *J. Org. Chem.* **1962**, *27*, 218−226.
(65) Dave, K. J.; Riley, C. M.; Vander Velde, D.; Stobaugh, J. F. *J. Pharm. Biomed. Anal.* **1990**, *8*, 307−312.
(66) Sauer, J. C. *Org. Synth. Coll. Vol. 4* **1963**, 813−815.
(67) L'Eplattenier, F.; Pugin, A. *Helv. Chim. Acta* **1975**, *58*, 917−929.

specifically, direct complexation with Fe^{III} salts in the presence of triphenylamine, air oxidation of preformed Fe^{II} complexes, and oxidation of preformed Fe^{II} complexes by the hexachloroantimonate salt of tris(*p*-bromophenyl)amine radical cation. Except for the air oxidation step, all steps of the following preparations were carried out with careful exclusion of oxygen and moisture under argon. All complexes have melting points of >350 °C. Only one procedure for each complex is given below; additional procedures are given in the Supporting Information.

Complex 1-Fe^{III}Cl. A mixture of anhydrous Fe^{II}-chloride (67.7 mg, 0.53 mmol) and triphenylamine (390 mg, 1.59 mmol) in dry THF (5 mL) was stirred for 15 h at ambient temperature. The brownish suspension was heated to 60 °C, and a solution of **1** (150 mg, 0.52 mmol) in dry THF (20 mL) was added within 5 min. After the mixture was stirred for 30 min at 60 °C, the argon flow was cut off and the mixture was stirred at room temperature for 15 h at the open air. The black precipitate was filtered off, washed two times with dry THF (2 mL each), and dried at 60 °C under vacuum to yield 168 mg (0.44 mmol, 73%) of the complex. Elemental analysis calcd (%) for $C_{18}H_{14}N_4FeCl$ (377.63): C, 57.25; H, 3.74; N, 14.84; Fe, 14.79. Found: C, 57.33; H, 3.66; N, 14.92; Fe, 13.25.

Complexes 2-Fe^{II}Cl·2THF and 2-Fe^{III}Cl·THF. A deoxygenated solution of **2** (416 mg, 0.96 mmol) in dry THF (20 mL) was added within 5 min to a rapidly stirred mixture of triphenylamine (720 mg, 2.94 mmol) and anhydrous iron(III) chloride (165 mg, 1.02 mmol) in dry THF (10 mL) at 60 °C. After being stirred for 30 min at 60 °C, the reaction mixture was kept at room temperature for 30 min, and the formed precipitate was separated on a D4 glas frit, washed twice with THF (2 mL each), and dried in vacuum at 60 °C to give 188 mg (0.28 mmol, 29%) of complex **2-Fe^{II}Cl·2THF**. The filtrate was stored at −30 °C for 4 d, after which a second precipitate was formed. This precipitate was isolated as before, affording 27 mg (0.05 mmol, 5%) of complex **2-Fe^{III}Cl·THF**. **2-Fe^{II}Cl·2THF**: Elemental analysis calcd (%) for $C_{24}H_{23}N_4O_4FeCl·(C_4H_8O)_2$ (666.17): C, 57.63; H, 5.89; N, 8.40; Fe, 8.37. Found: C, 57.48; H, 5.80; N, 8.30; Fe, 8.23. HRMS (ESI-TOF, MeOH): a signal for the undestroyed complex could not be detected. Calcd for $C_{24}H_{24}N_4O_4$ *m/z*: 432.1792 [M^+ − FeCl, − 2THF]. Found: 432.1831. **2-Fe^{III}Cl·THF**: Elemental analysis calcd (%) for $C_{24}H_{22}N_4O_4FeCl·C_4H_8O$ (593.86): C, 56.63; H, 5.09; N, 9.43; Fe, 9.40. Found: C, 56.58; H, 5.00; N, 9.40; Fe, 9.36. MS (ESI-TOF, MeOH) calcd for $C_{18}H_{14}N_4O_4FeOCH_3$ *m/z*: 517.1 [M^+ − THF, − $SbCl_6$, + OCH_3]. Found: 517.3. HRMS (ESI-TOF, MeOH) calcd for $C_{24}H_{22}N_4O_4FeCl$ *m/z*: 521.0679 [M^+ − THF]. Found: 521.0678. UV/vis (DMSO): λ_{max}(lg ϵ) = 317(4.17), 374-(4.27), ∼550(∼3.72), ∼770(∼3.60) nm.

Complex 3-$Fe^{III}SbCl_6$·2THF. A suspension of anhydrous $FeCl_2$ (42.0 mg, 0.33 mmol) in dry THF (10 mL) was stirred for 12 h at ambient temperature. Then, tris(*p*-bromophenyl)amine (453 mg, 0.94 mmol) was added, the mixture was heated to 50 °C, and a solution of **3** (210 mg, 0.31 mmol) in dry THF (20 mL) was added within 5 min. After the mixture was stirred at 60 °C for 40 min, a solution of tris(*p*-bromophenyl)ammonium hexachloroantimonate (277 mg, 0.34 mmol) in DMSO/THF 1:2 (v/v) (2 mL) was rapidly added, stirred for further 20 min at 60 °C, and cooled to room temprature. After 30 min of stirring at ambient temperature, deoxygenated *n*-hexane (10 mL) was added, and the formed black precipitate was filtered off, washed three times with dry THF/hexane (1:1 v/v) (5 mL each), and vacuum-dried to yield 179 mg (0.15 mmol, 48%) of **3-$Fe^{III}SbCl_6$·2THF**. Elemental analysis calcd (%) for $C_{44}H_{30}N_4O_4FeSbCl_6·(C_4H_8O)_2$ (1213.27): C, 51.48; H, 3.82; N, 4.62; Fe, 4.60. Found: C, 51.35; H, 3.81; N, 4.76; Fe, 4.58. HRMS (ESI-TOF, MeOH) calcd for $C_{44}H_{30}N_4O_4FeCl$ *m/z*: 769.1305 [M^+ − 2THF − $SbCl_6$ + Cl]. Found: 769.1344.

Complex 4-Fe^{III}Cl·THF. A deoxygenated solution of **4** (100 mg, 0.24 mmol) in dry THF (35 mL) was added within a period of 30 min to a rapidly stirred mixture of triphenylamine (180 mg, 0.074 mmol) and anhydrous iron(III) chloride (40 mg, 0.24 mmol) in dry THF (10 mL) at 60 °C. After the mixture was stirred for 12 h at ambient temperature, the black precipitate was separated on a glas frit and washed twice with cold, dry THF (5 mL each) and dried under vacuum to give 35.0 mg (0.06 mmol, 26%) of complex **4-Fe^{III}Cl·THF**. UV/vis (DMF): λ_{max} (lg ϵ) = 319(4.42), 372(4.56), 439(4.32), 466(4.21). Elemental analysis calcd (%) for $C_{22}H_{22}N_4O_4FeCl·C_4H_8O$ (569.84): C, 54.80; H, 5.31; N, 9.83; Fe, 9.80. Found: C, 54.66; H, 5.09; N, 9.62; Fe, 9.93. HRMS (ESI-TOF, MeOH) calcdd for $C_{22}H_{22}N_4O_4FeCl$ *m/z*: 497.0679 [M^+ − THF]. Found: 497.0680.

Complex 5-Fe^{III}Cl. To a rapidly stirred mixture of triphenylamine (126 mg, 0.513 mmol) and anhydrous Fe^{II}-chloride (24.5 mg, 0.193 mmol) in THF (5 mL) was added at 60 °C a solution of **5** (100 mg, 0.171 mmol) in THF (25 mL) over a period of 30 min. After being stirred for 30 min at 60 °C, the mixture was cooled to room temperature, the argon stream cut off, and the solution stirred for 15 h at the open air. The black precipitate was filtered off, washed four times with THF (5 mL each), and dried under vacuum. Yield: 95 mg (0.14 mmol, 82%). UV/vis (DMF): λ_{max} (lg ϵ) = 275(4.36), 375(4.35), 443(4.14), ∼520(∼3.78) nm. Elemental analysis calcd (%) for $C_{30}H_{38}N_4O_8FeCl$ (673.94): C, 53.47; H, 5.68; N, 8.31; Fe, 8.29. Found: C, 53.66; H, 5.55; N, 8.28; Fe, 8.21. HRMS (ESI-TOF, MeOH) calcd for $C_{30}H_{38}N_4O_8FeCl$ *m/z*: 673.1727 [M^+]. Found: 673.1744.

Complex 6-Fe^{III}Cl. To a rapidly stirred mixture of triphenylamine (91 mg, 0.37 mmol) and anhydrous Fe^{II}-chloride (17.3 mg, 0.124 mmol) in THF (5 mL) was added at 60 °C a solution of **7** (100 mg, 0.124 mmol) in THF (25 mL) over a period of 30 min. After being stirred for 30 min at 60 °C, the mixture was cooled to room temperature, the argon stream cut off, and the solution stirred for 15 h at the open air. The black precipitate was separated by centrifugation, washed four times with THF (5 mL each), and dried under vacuum. Yield: 75 mg (0.084 mmol, 67%). Elemental analysis calcd (%) for $C_{42}H_{54}N_4O_{12}FeCl$ (898.2): C, 56.16; H, 6.06; N, 6.24; Fe, 6.22. Found: C, 56.06; H, 6.00; N, 6.36; Fe, 6.15. MS (ESI-TOF, MeOH): a signal deriving from the complex could not be detected. Calcd for $C_{42}H_{56}N_4O_{12}$ *m/z*: 808.4 [M^+ − FeCl, + 2H]; found 808.5.

EPR Measurements. X-band (9.5 GHz) EPR spectra were recorded at 77 K from solid samples or 1−5 mM frozen DMSO solutions in 4 mm o.d. quartz tubes immersed in a liquid nitrogen Dewar insert in a TM_{110} wide-bore cavity. Instrument settings: sweep range, 400 mT; modulation amplitude, 1 mT; modulation frequency, 100 kHz; sweep time, 15 min. Spectral simulations were carried out with the Simfonia program (Bruker).

Mössbauer Measurements. Mössbauer data were recorded on an alternating constant-accelaration spectrometer. The minimum experimental line width was 0.24 mm s^{-1} (full width at half-height). The sample temperature was maintained constant in an Oxford Instruments Variox cryostat. Isomer shifts are quoted relative to iron metal at 300 K.

Magnetic Susceptibility Measurements. The solid-state magnetic susceptibilities were measured from 290 to 1.9 K at a magnetic field of 1.0 T by the SQUID method.

Oxygen Measurements. Aliquots of 5 mM DMSO stock solutions of the iron complexes were added to phosphate buffer solutions (10 mL, 50 mM, pH 7.2−7.3, 21 °C) in the reaction

Scheme 2. Synthesis of Ligands **2**−**6**[a]

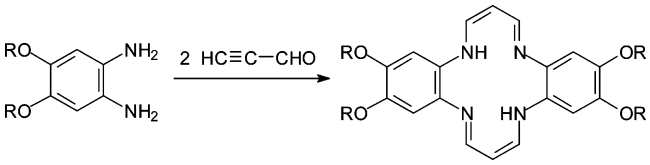

[a] R = CH_3, $C(CH_3)_2$, $C(C_6H_5)_2$, $CH_2CH_2OCH_3$, $CH_2COOtBu$.

chamber of a Clark-type oxygen electrode unit to give final concentrations of 0.5−20 μM. The local platinum electrode disc underneath the reaction chamber and a membrane serves as the floor of the reaction chamber. The membrane is sufficiently permeable to permit diffusion of oxygen from the contents of the reaction chamber while remaining impermeable for the products of the oxygen reduction reaction which occur at the platinum electrode. The release of O_2 was started by adding H_2O_2 (final concentrations 100 or 250 μM) to the reaction chamber, and the instantaneously released amount of molecular oxygen was quantified polarographically with the oxygen electrode which was calibrated according to the instructions of the manufacturer.

Results

Syntheses of Ligands. The ligands are prepared following the synthesis for the unsubstituted 5,14-dihydro-5,9,14,18-tetraaza-dibenzo[*a*,*h*]cyclotetradecene (**1**), i.e., *o*-phenylenediamine is reacted with propinal.[45] This one-pot reaction generally leads to 5,14-dihydro-5,9,14,18-tetraaza-dibenzo-[*a*,*h*]cyclotetradecene and its substituted derivatives in yields of 20−45%. The reactions are run in dry ethanol under argon, and precautions have to be taken to exclude oxygen and moisture from the reaction.

The side chains in ligands **3**, **5**, and **6** are designed in order to suppress possible formation of μ-oxo complexes due to steric interactions of the bulky phenyl groups (**3**), to increase the water solubility (**5**), and to obtain a cell membrane-permeable, esterase-hydrolyzable[68] Fe^{III} complex (**6**). The synthesis of the substituted derivatives **2**−**6** (Scheme 2) starts from bis-*o*-substituted hydroquinones. After double nitration in two consecutive steps, catalytic reduction is carried out in dry and oxygen-free THF using palladium on charcoal. Reduction to the 1,2-diamines is quantitative as checked by ^{1}H NMR spectroscopy. The diamines are highly air sensitive, so that no further purification is carried out and macrocyclization with propinal is performed on the crude product.

Preparation of Iron(III) Complexes. Iron(III) complexes of tetraazamacrocyclic ligands are commonly prepared by oxidation of the corresponding Fe^{II} complexes formed from reaction of the ligand with an iron(II) salt. This strategy is based on the presumption that the "soft" Fe^{II} ion is a better partner for nitrogen ligands than the "hard" Fe^{III} ion. The Fe^{II} complexes of aza macrocycles are highly air sensitive and can be handled only in an inert atmosphere. Easy oxidation to the Fe^{III} complexes has been achieved by molecular oxygen[69,70] or by iodine[71] There are, however, also

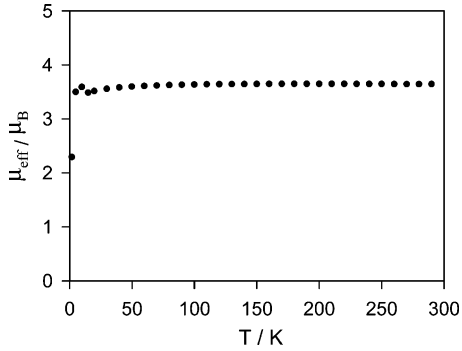

Figure 1. Temperature dependence of the effective magnetic moment of **3-Fe^{III}SbCl$_6$·2THF** in the solid state.

examples where Fe^{III} has been directly coordinated to the ligand.[51] Several approaches were tested to obtain the Fe^{III} complexes of ligands **1**−**6**, which will be described in the following.

Complex **2-Fe^{III}BF$_4$** was previously prepared by reacting Fe^{II} acetate or Fe^{II} chloride with **2** and oxidizing the resulting Fe^{II} complex by bubbling molecular oxygen through its THF suspension in the presence of tetraethylammonium tetrafluoroborate (Scheme 3). In the most successful of these preparations it was possible to isolate 48% of **2-Fe^{III}BF$_4$**. However, this procedure turned out not to be very reproducible. A more gentle oxidation by molecular oxygen leads to reproducible, higher yields of the Fe^{III} complexes. Oxidation is performed under controlled condition, i.e., the Fe^{II} complex, as prepared under an argon atmosphere, is exposed to oxygen simply by letting air diffusing into the reaction vessel for several hours through a small hole. The then-formed precipitate is filtered off and analyzed. By this means it was possible to isolate **1-Fe^{III}Cl** in 73%, **2-Fe^{III}Cl** in 90%, **3-Fe^{III}Cl** in 18%, **4-Fe^{III}Cl** in <10%, **5-Fe^{III}Cl** in 82%, and **6-Fe^{III}Cl** in 67% yield.

In a second approach, the preformed Fe^{II} complex is oxidized by the one-electron oxidant tris(4-bromophenyl)-aminium hexachloroantimonate. A THF solution of the ligand and slightly more than two equivalents of tris-(4-bromophenyl)amine are reacted with iron(II) chloride or iron(II) acetate to obtain the Fe^{II} complexes; the reaction mixture is then treated in situ with one equivalent of tris(4-bromophenyl)-aminium hexachloroantimonate. The complexes precipitate either as hexachloroantimonate, or chloride salt, or a mixture of both. Noteworthy, the complexes prepared via this route contain two equivalents of the solvent THF, as established by elemental analyses and ^{1}H NMR spectrometric analysis of their DMSO solutions. By this means **1-Fe^{III}SbCl$_6$·2THF**, **2-Fe^{III}Cl·2THF**, and **3-Fe^{III}SbCl$_6$·2THF** are obtained in 30, 52, and 48% yield, respectively. The complexes show correct molecular masses in their ESI-TOF mass spectra. Signals due to the free ligands could not be detected.

On first sight, a more straightforward way to the Fe^{III} complexes would be the direct complexation of iron(III) salts. Our initial attempts to use iron(III)chloride in THF in the presence of triethylamine as base to scavenge the hydro-

(68) Meineke, P.; Rauen, U.; de Groot, H.; Korth, H.-G.; Sustmann, R. *Chem.—Eur. J.* **1999**, *5*, 1738−1747.
(69) Karn, J. L.; Busch, D. H. *Inorg. Chem.* **1969**, *8*, 1149−1153.
(70) Melnyk, A. C.; Kildahl, N. K.; Rendina, A. R.; Busch, D. H. *J. Am. Chem. Soc.* **1979**, *101*, 3232−3240.
(71) Jäger, E. G.; Keutel, H.; Rudolph, M.; Krebs, B.; Wiesemann, F. *Liebigs Ann. Chem.* **1995**, 503−514.

Scheme 3. Preparation of Complex **2-Fe^{III}BF$_4$**

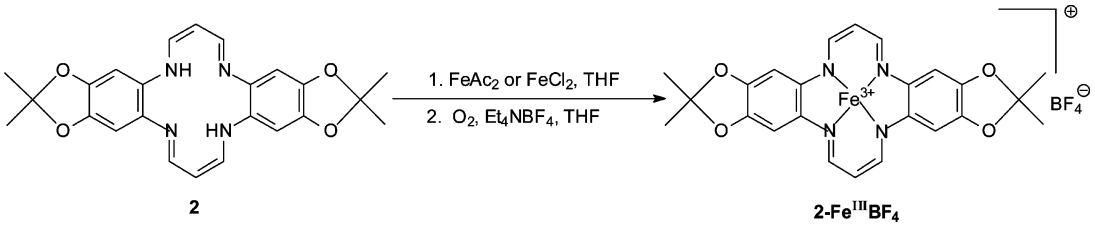

chloric acid were unsuccessful. The use of tri-*n*-octylamine as a more lipophilic base did not improve isolation of the desired complex. Only when triphenylamine was applied in slight excess (3 equiv) could a useful procedure be worked out, but the yields are low to moderate (5−30%). The solid complexes obtained by this means are either solvent-free (**1-Fe^{III}Cl**) or contain one (**2-Fe^{III}Cl·THF**, **4-Fe^{III}Cl·THF**) or two equivalents of THF (**3-Fe^{III}Cl·2THF**, **5-Fe^{III}Cl·2THF**, **6-Fe^{III}Cl·2THF**).

Among the experiments of direct complexation with iron(III) chloride, a unique observation is made with the acetonide ligand **2**: Immediately after addition of a solution of $FeCl_3$ in THF to an equimolar THF solution of **2** in the presence of triphenylamine, a dark-brown 1:1 Fe-ligand chloride salt precipitates in ca. 30% yield. This product unexpectedly turns out to be an Fe^{II} high-spin ($S = 2$) complex (**2-Fe^{II}Cl·2THF**) (see Mössbauer spectrum, Supporting Information, Figure S6), revealing that iron(III) is reduced in the course of the reaction. Allowing the mother liquor of such an experiment to stand overnight at −18 °C provides a second fraction of an almost black 1:1 complex, identified as **2-Fe^{III}Cl·THF**, in ca. 5% yield. Both solids give correct elemental analyses (see Experimental Section), but differ strongly in their spectroscopic and ESI mass spectrometric characteristics as well as in the reaction with hydrogen peroxide (see below). The second precipitate shows high-intensity signals of masses **2** + Fe and **2** + Fe + Cl but none of the bare ligand **2**, whereas the ESI mass spectrum of the initial precipitate **2-Fe^{II}Cl·2THF** shows mainly the signal of the molecular ion of the bare ligand but none of an iron complex.

Electronic Absorption Spectra. The UV/vis spectra of ligands **1**−**6** in organic solvents and in aqueous solution all show a characteristic, strong three-band pattern, consisting of a narrow band around 270 nm and two twin bands around 365 nm and in the 430−480 nm range, with maxima separated by 10−12 and 20−25 nm, respectively (Table S1 and Figure S1a, Supporting Information). The position of the 270 and 365 nm bands is largely independent of the substitution pattern of the parent macrocycle, whereas the positions of the long-wavelength maxima differ by about 20−25 nm for the various substituents. Weaker, unresolved shoulders extend down to ca. 800 nm. The distinct three-band pattern of the free ligands **1**−**6** is largely lost in the absorption spectra of the corresponding iron(III) complexes **1-Fe^{III}Cl**−**5-Fe^{III}Cl** (Figure S1b). No remarkable difference among the spectra of the individual complexes is recognizable. The intense, broad spectra show two maxima at 315 and at 360−380 nm; weaker, unresolved absorptions can be identified in the 500−600 and 650−800 nm region, respectively, which are reasonably attributed to the Fe-ligand CT bands. In some preparations, two weaker, narrow absorptions are detected around 515 and 545 nm (see Figure S1b). These absorptions are accompanied by a narrow, isotropic single line at $g \approx 2.00$ in the related EPR spectra (see below). Since these absorptions are not detected in aqueous solution, a hydrolytic degradation of the related species is inferred.

In marked contrast to the absorption spectra of **1-Fe^{III}Cl**−**5-Fe^{III}Cl**, the spectra of the Fe^{II} complex **2-Fe^{II}Cl** and the Fe^{III} complex **6-Fe^{III}Cl** are almost indistinguishable to the spectra of their parent ligands **2** and **6**, respectively (Figure S1a) although the elemental analyses gave correct percentages for one equivalent of iron. This fact implies that the iron ion exerts only a weak electronic interaction with the macrocyclic ligand (see Discussion).

Magnetic Susceptibilities. In order to establish the spin states of the iron center in our catalytically active complexes, the magnetic susceptibilities in the solid state were measured by SQUID magnetometry in the temperature range from 1.9 to 290 K at a field of 1.0 T for a few selected complexes. The solvent-free complex **3-Fe^{III}Cl** shows a slightly curved dependence of the inverse molar susceptibility χ_m^{-1} on temperature (see Supporting Information, Figure S2a). Accordingly, the effective magnetic moment μ_{eff} decreases slightly from a room temperature value of 3.47 to ca. $2.9\mu_B$ at 10 K (Figure S2b). The magnetic moment is somewhat lower than the "spin-only" value $3.87\mu_B$ as expected for the intermediate ($S = {}^3/_2$) spin state of a pentacoordinate Fe^{III} complex of that kind.[72] With regard to the preparation procedures (see above) and the handling of the samples in contact with air, the μ_{eff} lower than the spin-only value can reasonably be attributed to contamination by residual parent Fe^{II} low-spin ($S = 0$) complex, Fe^{III} low-spin ($S = {}^1/_2$) species, and/or the admixture of superparamagnetic, antiferromagnetically coupled iron oxide impurities, formed by reaction with atmospheric oxygen (compare related Mössbauer spectra, below).

Complex **3-Fe^{III}SbCl$_6$·2THF** strictly obeys the Curie−Weiss law down to 10 K (Figure S3). The effective magnetic moment $\mu_{eff} = 3.64\mu_B$ is independent of the temperature between 290 and 10 K (Figure 1). According to its Mössbauer spectrum (see below), this sample contains about 16% admixture of a different spin-state component, which may be due to low-spin Fe^{III} or a mixture of high-spin Fe^{III} and low-spin Fe^{II}. Complex **2-Fe^{III}Cl·2THF** also shows a linear

(72) Keutel, H.; Käpplinger, I.; Jäger, E.-G.; Grodzicki, M.; Schünemann, V.; Trautwein, A. X. *Inorg. Chem.* **1999**, *38*, 2320−22327.

Table 1. Mössbauer Spectroscopic Data at 80 K in the Solid State

compound	δ [mm s^{-1}][a]	ΔE_Q [mm s^{-1}][b]	spin state	%
1-Fe^{III}SbCl$_6$·2THF	0.20	3.16	Fe^{III}, $S = 3/2$	61
	0.25	2.73	Fe^{III}, $S = 3/2$ or $1/2$	20
	0.38	0.51	Fe^{III}, $S = 5/2$	19
2-Fe^{III}Cl·2THF	0.22	3.20	Fe^{III}, $S = 3/2$	94
	0.43	0.46	Fe^{III}, $S = 5/2$	6
2-Fe^{III}Cl	0.46	0.88	Fe^{III}, $S = 5/2$	46
	0.22	3.10	Fe^{III}, $S = 3/2$	43
	0.25	2.26	Fe^{III}, $S = 3/2$ or $1/2$	11
2-Fe^{II}Cl·2THF	1.01	1.61	Fe^{II}, $S = 2$	>95
3-Fe^{III}Cl	0.20	3.08	Fe^{III}, $S = 3/2$	81
	0.34	0.25	Fe^{III}, $S = 5/2$ or Fe^{II}, $S = 0$	19
3-Fe^{III}SbCl$_6$·2THF	0.19	2.95	Fe^{III}, $S = 3/2$	47
	0.20	3.14	Fe^{III}, $S = 3/2$	37
	0.37	0.28	Fe^{III}, $S = 5/2$ or Fe^{II}, $S = 0$	16
3-Fe^{III}SbCl$_6$·2THF	0.19	3.01	Fe^{III}, $S = 3/2$	88
	0.30	0.41	Fe^{III}, $S = 5/2$	12
5-Fe^{III}Cl	0.53	0.99	Fe^{III}, $S = 5/2$	46
	0.08	1.72	Fe^{III}, $S = 1/2$	22
	0.29	1.20	Fe^{III}, $S = 5/2$	21
	0.20	2.95	Fe^{III}, $S = 3/2$	11
6-Fe^{III}Cl	0.46	0.67	Fe^{III}, $S = 5/2$[c]	>95

[a] Isomer shift relative to α-Fe at room temperature. [b] Quadrupole splitting. [c] Spectrum is broadened by intermediate paramagnetic relaxation. The pattern was approximated by an asymmetric Lorentzian doublet.

dependence of χ_m^{-1} on the temperature down to ca. 10 K. The effective magnetic moment μ_{eff} varies sligthly from 3.36 to 3.10μ_B between 290 and 100 K (Figure S4). In conclusion, the susceptibility data confirm that the Fe^{III} center of the pentacoordinate, catalytically active complexes is of intermediate spin in the solid state and that this spin state is largely preserved even in the presence of two additional solvent molecules per formula unit.

Mössbauer Spectra. The oxidation and spin states of the complexes are further examined by zero-field Mössbauer spectra, recorded at 80 K from powder samples. It appears that most of the preparations of the catalsysts are mixtures of different spin states of iron(III) and iron(II) at varying ratios. The spectral parameters, evaluated by fitting to overlapping Lorentzian doublets, are summarized in Table 1. The spectra of all preparations which show high catalase-like activity (see below), are dominated by doublet signals with isomer shifts in the range of $\delta = 0.19-0.25$ mm s^{-1} and quadrupole splittings of $\Delta E_Q = 2.7-3.2$ mm s^{-1}. A typical example is shown in Figure 2. Although the numeric ranges of these parameters are in accord with previous reports on intermediate-spin Fe^{III} complexes with very similar ligand coordination,[72] they do not allow an unequivocal discrimination between the doublet and quartet spin states. However, from the magnetic susceptibility measurements described above it follows that they have to be attributed to the intermediate-spin ($S = 3/2$) state. Figures of Mössbauer spectra of some other complexes and related discussion are given in the Supporting Information, Figures S5−S10.

Essentially identical spectra are obtained for material prepared by gentle oxidation of the parent Fe^{II} complex by molecular oxygen or by one-electron oxidation of the Fe^{II} complex with tris(4-bromophenyl)aminium hexachloroantimonate. If, however, the complex is prepared by reaction of **2** with iron(III) chloride in the presence of triphenylamine, its Mössbauer spectra display features which strongly depend on the workup procedure. As noted above, a complex (**2-Fe^{II}Cl·2THF**) is initially isolated which unexpectedly shows the characteristic Mössbauer parameters of an iron(II) high-spin ($S = 2$) system (Figure S6). This is quite unusual as an Fe^{II} complex of ligand **2** should be a neutral species, i.e., should not be associated with a chloride counterion. The structure of **2-Fe^{II}Cl·2THF** and the purported role of triphenylamine in these preparations is discussed below. On delayed workup, varying mixtures of this high-spin iron(II) complex and the desired intermediate-spin Fe^{III} complex **2-Fe^{III}Cl** are obtained until after prolonged standing (24 h) of the mother liquor the almost pure Fe^{III} intermediate-spin complex **2-Fe^{III}Cl·2THF** (Figure 2) is obtained in low yield.

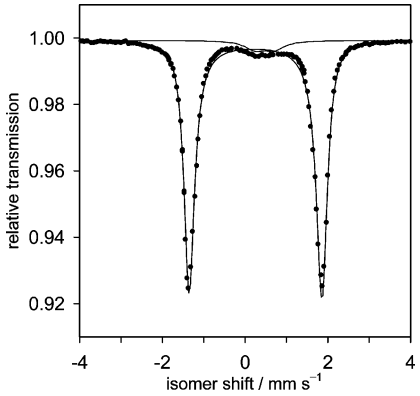

Figure 2. Solid-state Mössbauer spectrum of **2-Fe^{III}Cl·2THF** at 80 K. The spectrum is analyzed (solid lines) as a mixture of 94% intermediate-spin and 6% high-spin iron(III).

Despite the fact that in some preparations (see Table 1) a major contribution of Fe^{III} high-spin complexes is detected, which are found to be catalytically inactive, the preparations still show good catalase-like activity (see below).

Complex **6-Fe^{III}Cl**, which was designed as a catalyst being capable of penetrating cell membranes, turns out to be an almost pure Fe^{III} high-spin complex (Figure S10) that shows no activity with respect to hydrogen peroxide decomposition (see below).

The Mössbauer data of Table 1 confirm the conclusion from the susceptibility data that inclusion of THF solvent molecules does not affect the intermediate spin state of the catalytically active complexes in the solid state.

EPR Spectra. The EPR spectra of the catalytically active preparations of complexes **1-Fe^{III}**−**5-Fe^{III}** in the solid state at 293 and 77 K are dominated by very broad, strongly anisotropic signals in the $g \approx 2$ region which allow no unambiguous identification of the spin state. For a correlation of the spin state of the Fe^{III} complexes with their catalase-like activity, aqueous-phase spectra would be desirable. Unfortunately, the solubility of the present complexes in nonpolar organic solvents as well as in water is too low to achieve a suffcient signal intensity. Therefore, EPR spectra are recorded in glassy DMSO matrix at 77 K (Supporting Information, Figure S11, Table S2). All EPR spectra show

Table 2. Oxygen Production, Second-Order Rate Constants of Oxygen Release, and Catalytic Turnover Numbers of Hydrogen Peroxide Decomposition by Iron(III) Complexes[a]

entry	complex[b]	method of preparation	O_2 yield [%][c]	$k(Fe^{III} + H_2O_2)$ [M^{-1} s^{-1}]	TON[d]
1	**1-Fe^{III}Cl**	$FeCl_3$ + triphenylamine	75	1268 ± 41	41 ± 8
2	**1-Fe^{III}SbCl$_6$·2THF**	$FeCl_2$ + triphenylamine radical cation	83		
3	**1-Fe^{III}Cl**	$FeCl_2$ + air	72		
4	**2-Fe^{II}Cl·2THF**	$FeCl_3$ + triphenylamine, first precipitate	8		
6	**2-Fe^{III}BF$_4$**	$FeCl_2$ + air	87	1528 ± 104	79 ± 14[e]
7	**2-Fe^{III}Cl·THF**	$FeCl_3$ + triphenylamine, second precipitate	70		
8	**2-Fe^{III}SbCl$_6$·2THF**	$FeCl_3$, triphenylamine radical cation	80	1533 ± 68	74 ± 5
9	**2-Fe^{III}Cl**	$FeCl_2$ + air	80		
10	**3-Fe^{III}Cl·2THF**	$FeCl_3$ + triphenylamine	75		55 ± 5
11	**3-Fe^{III}SbCl$_6$·2THF**	$FeCl_2$ + triphenylamine radical cation	85		
12	**3-Fe^{III}Cl**	$FeCl_2$ + air	73	2336 ± 86	
13	**5-Fe^{III}Cl·2THF**	$FeCl_3$ + triphenylamine	70	1578 ± 66	52 ± 7
14	**5-Fe^{III}Cl**	$FeCl_2$, + air	82		
14	**6-Fe^{III}Cl·2THF**	$FeCl_3$ + triphenylamine	0		
16	**6-Fe^{III}Cl**	$FeCl_2$ + air	0		

[a] 100 μM H_2O_2, 5 μM Fe complex, phosphate buffer pH 7.3, T = 21 °C. [b] Notation indicates solid-state composition. [c] According to the stoichiometry of native catalase. [d] TON (turnover number) = mol H_2O_2 decomposed/mol catalyst. [e] Ref 52.

the characteristic features of low- and high-spin Fe^{III} in the $g = 2$ and $g = 4-9$ region, respectively, The relative intensity of the low- and high-spin signals varies strongly among the various preparations. However, although the spectra are better resolved than those from the polycrystalline material, they appear unusually weak with regard to the applied concentrations (2−5 mM), as deduced from comparison with similarly concentrated DMSO solutions of pure Fe^{III} high- and low-spin complexes.

The best spectral resolution is obtained for **2-Fe^{III}Cl·2THF**, prepared by oxidation of the corresponding **2**-Fe^{II} complex with the triphenylaminium radical cation salt, showing a rhombic g tensor with $g_1 = 2.26$, $g_2 = 2.15$, and $g_3 = 1.97$ as typical for low-spin Fe^{III} (Figure S11b). The other complexes also show low-spin Fe^{III} signals with very similar g-values, although the broader, less resolved signals (Figure S11a,c) suggest the overlap of several similar spectra. This may arise from inhomogeneous distribution of the molecules in the matrix, conformational effects of the side chains, and/or a varying coordination by DMSO. The EPR spectrum of **6-Fe^{III}Cl** (Figure S11d) shows only high-spin signals in addition to a strong, isotropic $g = 2$ singlet (see below). Surprisingly, in no case signals which may reasonably be attributed to intermediate-spin ($S = {}^3/_2$) Fe^{III} species are detected. Hence, it must be assumed that even in the rather dilute DMSO matrix magnetic interactions between the paramagnetic molecules take place which render the $S = {}^3/_2$ spin state of our complexes EPR-silent. Therefore, it seems that the observed EPR signals are only due to minor fractions of low- and high-spin Fe^{III} species already present in the solid samples and/or formed by coordination of DMSO (see Discussion).

A possible "spin-crossover" equilibrium between the $S = {}^1/_2$ and $S = {}^5/_2$ states is unlikely, because the DMSO matrix spectra from various preparations of the same complex show varying relative signal intensities of the low- and high-spin Fe^{III} resonances. In case of a spin-crossover equilibrium, one would expect the same ratio of the signal intensities from the different preparations after having stored their DMSO solutions for some time at room temperature prior to freezing. This is not the case.

Noteworthy, in some preparations an additional, sharp isotropic singlet ($\Delta B_{pp} = 1.5-2.0$ mT) at $g \approx 2.001$ is observed (Figure S11b−d). This signal, the intensity of which varies strongly with the method of preparation of the complex and the workup procedure, is the most intense feature of the EPR spectra of **2-Fe^{II}Cl·2THF** and **6-Fe^{III}Cl**, and it is accompanied by the appearance of electronic absorption bands at $\lambda_{max} = 515$ and 545 nm in the UV/vis spectra (see above).

Reaction with Hydrogen Peroxide. In a preliminary communication we demonstrated that **2-Fe^{III}BF$_4$** decomposes hydrogen peroxide to oxygen and water at pH values and concentration ranges typically found in physiological systems.[52] The catalase-like activity was established by electrochemically monitoring (Clark-type electrode) the release of O_2 at 25 °C in 50 mM phosphate buffer at pH 7.2. On the basis of the catalase-like stoichiometry, a production of 87% O_2 (relative to H_2O_2) and a catalytic turnover number (TON) of about 79 were determined. The catalase-like activity of Fe^{III} complexes **1-Fe^{III}X·*n*THF**−**6-Fe^{III}X·*n*THF** (X = Cl, $SbCl_6$; n = 0, 1, 2) and Fe^{II} complex **2-Fe^{II}Cl·2THF** is examined by the same electrochemical method (Table 2). To this end, a standardized procedure is applied where the decomposition of a 100 μM solution of hydrogen peroxide to oxygen is measured in phosphate buffer pH 7.3 in the presence of 5 μM of the iron complex. Although all preparations of the iron(III) complexes give satisfying iron elemental analyses, their efficacy of oxygen production from hydrogen peroxide, in terms of both kinetics and yield, varies with the method of preparation (see Table 2). The chloride and hexachloroantimonate salts **2-Fe^{III}Cl·THF** and **2-Fe^{III}SbCl$_6$·2THF** are investigated in order to establish whether the counterion would have any effect on the reactivity.

Complexes **2-Fe^{III}Cl**, **2-Fe^{III}Cl·THF**, and **2-Fe^{III}SbCl$_6$·2THF** are found to be of similar activity toward H_2O_2 (70−80% O_2 production, see Table 2) as the previously investigated tetrafluoroborate salt **2-Fe^{III}BF$_4$**.[52] For comparison

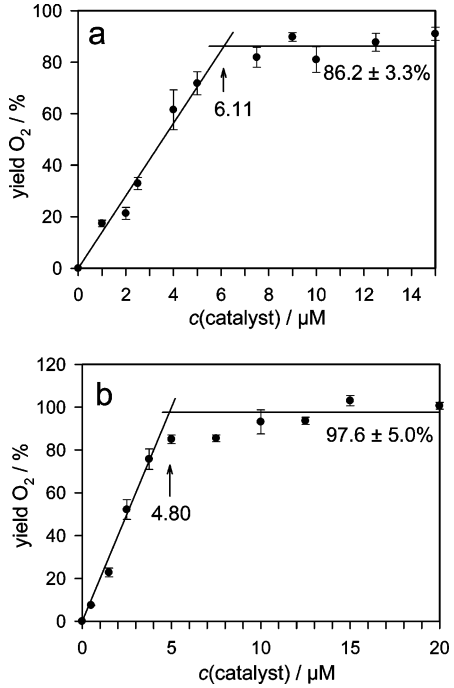

Figure 3. Oxygen yield (%) according to catalase stoichiometry as a function of the catalyst concentration from reaction of 250 μM hydrogen peroxide with (a) **1-Fe^{III}Cl** and (b) **5-Fe^{III}Cl** in phosphate buffer at pH 7.24 and $T = 21$ °C.

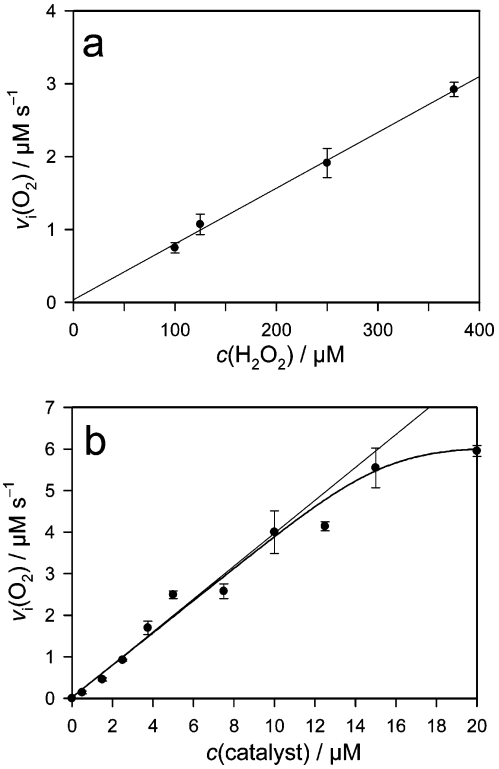

Figure 4. (a) Dependence of the initial rate of oxygen release on the concentration of H_2O_2 catalyzed by **1-Fe^{III}-Cl** (5 μM) (phosphate buffer pH 7.3, $T = 25$ °C). (b) Dependence of the initial rate of oxygen release from H_2O_2 (250 μM) on the concentration of **5-Fe^{III}Cl** (phosphate buffer pH 7.2, $T = 25$ °C).

purposes, **2-Fe^{II}Cl** is also tested for its catalase activity. In line with the expected propensity of Fe^{II} to react with H_2O_2 in terms of a Fenton reaction, H_2O_2 is indeed stoichiometrically decomposed but only minor amounts of oxygen are released, presumably because of some contamination by **2-Fe^{III}Cl**. Iron(III) complexes **3-Fe^{III}X·*n*THF**−**5-Fe^{III}X·*n*THF** are of similar activity as **2-Fe^{III}X·*n*THF**. Noteworthy, the Fe^{III} complex of ligand **1**, which initially was expected to be of reduced catalase-like activity due to the lack of additional electron-releasing substituents on the macrocycle, also produces oxygen in comparable yields to the oxygen-substituted derivatives. The sole completely inactive Fe^{III} complex found is **6-Fe^{III}Cl·2THF**. The reason for its inertness is discussed below.

For selected complexes, turnover numbers (TON), i.e., the moles of produced oxygen per mole of catalyst are determined. The TONs are evaluated from a plot of the catalyst concentration vs the oxygen yield using a fixed concentration of 250 μM of hydrogen peroxide in phosphate buffer pH 7.24. For low concentrations of the complexes, in the range 0−5 μM, oxygen release is linearly dependent on the catalyst concentration to approach a constant value above ca. 6 μM. The turnover numbers (Table 2) are calculated from the catalyst concentration at the crossing point of the two straight lines fitted to the data, as shown for example in Figure 3. As can be seen from Table 2, the TONs of the active complexes are quite similar, differing by only a factor of 2.

In the majority of these experiments, the constant production of oxygen at higher catalyst concentrations does not reach the expected 100% as obtained with native catalase. Typical maximum yields are in the 70−85% region, with the exception of **5-Fe^{III}Cl** for which the conversion of hydrogen peroxide to oxygen approaches 100% at higher catalyst concentration (Figure 3b).

As reported previously, for a fixed concentration of **2-Fe^{III}BF$_4$** the oxygen yield was found to be linearly dependent on the H_2O_2 concentration.[52] The same is true for **1-Fe^{III}Cl** (Supporting Information, Figure S12). In both cases, the slope of the regression line is close to a value of 0.5 as expected for a catalase-like stoichiometry. Measurements of the initial pseudo-first-order rates v_i of oxygen release as a function of the H_2O_2 concentration proved a first-order dependence on $c(H_2O_2)$ for the **2-Fe^{III}BF$_4$**-catalyzed reaction.[52] The same is observed for the unsubstituted complex **1-Fe^{III}-Cl** (Figure 4a). Thus, oxygen substitution of the macrocylic ligand does not seem to alter the apparent reaction order of H_2O_2 decomposition, and it can safely be assumed that a first-order dependence on $c(H_2O_2)$ also holds for the other catalytically active complexes of this study.

A similar picture is obtained when the initial pseudo-first-order rates of oxygen release at a constant hydrogen peroxide concentration of 250 μM are plotted against the concentration of the catalysts, as shown in Figure 4b for **5-Fe^{III}Cl**. Below 10 μM catalyst concentration, the initial rate is linearly dependent on the concentration of the iron(III) complex, as expected for a catalytic process. Thus, the rate-limiting step of H_2O_2 disproportionation is a second-order process, i.e., first-order in both catalyst and H_2O_2 concentration. From the slope of the plots as shown in Figure 4 (Figures S12−S14), second-order rate constants k(**L-Fe^{III}X** + H_2O_2) are obtained for **1-Fe^{III}Cl**, **2-Fe^{III}SbCl$_6$**, **2-Fe^{III}Cl**, **3-Fe^{III}Cl**, and **5-Fe^{III}Cl**

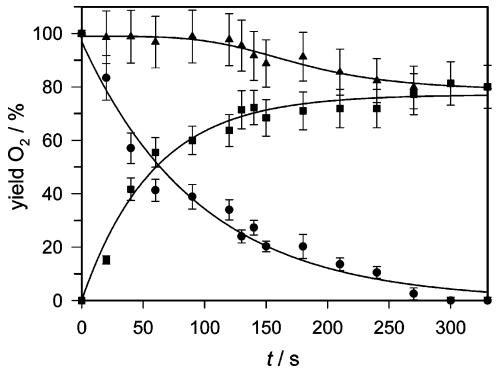

Figure 5. Time dependence of percentage oxygen release from decomposition of 100 μM hydrogen peroxide in the presence of 5 μM **2-Fe^{III}Cl** and catalase at pH 7.3 and 25 °C. Squares: oxygen production induced by **2-Fe^{III}Cl**; triangles: total yield of oxygen after addition of native catalase to the reaction mixture; circles: percentage amount of residual hydrogen peroxide not decomposed by **2-Fe^{III}Cl**.

(Table 2). However, as evident from Figure 4b, at $c(H_2O_2)$/c(catalyst) ratios below 35−25:1 the rate acceleration is increasingly diminished to approach more or less a constant value. This holds for all complexes investigated here.

These observations indicate that a side reaction takes place which decomposes hydrogen peroxide without release of molecular oxygen but which is obviously not the deactivation process of the catalyst coupled to the catalytic cycle. A series of experiments is carried out with **2-Fe^{III}Cl**, in which the release of O_2 from 100 μM hydrogen peroxide in the presence of 5 μM of the catalyst in phosphate buffer pH 7.3 and 25 °C is determined as a function of time. After mixing of the reactants, native catalase is added at increasing time intervals in order to determine the amount of undecomposed H_2O_2 in the reaction mixture at this stage of the reaction. The sum of the oxygen generated by the catalyst and by the added catalase allows the determination of the fraction of hydrogen peroxide that is decomposed without release of molecular oxygen. As can be deduced from Figure 5, up to about 50 s after starting the reaction, the total yield of oxygen is close to 100%. This demonstrates that initially no other pathway of hydrogen peroxide decomposition than the catalase-like one is followed. However, after about 60% decomposition of H_2O_2, the total oxygen production continuously diminishes to approach asymptotically a yield of ca. 80%, i.e. the maximum value determined for the catalyst alone (see Table 2). The total hydrogen peroxide decomposition can be estimated from these data (Figure 5, circles), proving that hydrogen peroxide is indeed completely decomposed after 300 s. Hence, after completion of the reaction, about 20% of H_2O_2 has been destroyed without producing oxygen. This confirms the above-mentioned presence of an additional, non-catalase-like reaction channel for decomposition of hydrogen peroxide.

Discussion

In the present study, Fe^{III} complexes of 5,14-dihydro-5,9,-14,18-tetraaza-dibenzo[*a*,*h*]cyclotetradecene **1** and substituted derivatives thereof (**2**−**6**) are prepared and tested for their ability to degrade hydrogen peroxide to oxygen and water, thus mimicking the function of the enzyme catalase. As boundary conditions for a compound considered to be a true catalase mimic, we define that the decomposition of hydrogen peroxide should obey the overall stoichiometry of catalase (eq 1) and that the reaction should take place in aqueous solution of ca. pH 7, at ambient temperature, and at micromolar concentrations of the catalyst and hydrogen peroxide, i.e., at conditions found in physiological envireonment. Several porphyrin-based Fe^{III} complexes and Fe(II/III) complexes of non-heme ligands have been prepared in the past and claimed to be catalase mimics. However, none of these compounds satisfies the above definition in all aspects.[15,18,36,73,74]

The preparation of the tetraazamacrocyclic ligands is straightforward, however, and normally gives only moderate yields in the range of 20 to 40%. Complexation of the ligands by Fe^{III} can be carried out in different ways. Although direct complexation with Fe^{III} salts is possible in the presence of triphenylamine, but not trialkylamines, the more satisfying procedures involve reaction with Fe^{II} salts and subsequent oxidation of the initially formed Fe^{II} complex. Since the Fe^{II} complexes are highly oxygen-sensitive, air oxidation is the method of choice. However, this process has to be carried out carefully, i.e., the oxygen level has to be maintained low in order to prevent oxidative degradation of the ligands. In the absence of air, oxidation of preformed Fe^{II} complexes can be performed by addition of equimolar amounts of the one-electron oxidant tris-4-bromophenylaminium hexachloroantimonate. Interestingly, the three complexation procedures provide solid material which differs by the number of incorporated solvent molecules, THF, per molecule of the Fe^{III} complex. Careful air oxidation of the preformed Fe^{II} complexes provides solvent-free products, whereas tris-4-bromophenylaminium hexachloroantimonate oxidation always gives complexes containing two equivalents of THF. By way of contrast, direct complexation with iron(III) chloride yields products of a varying number (0−2) of additional THF molecules per formula unit, depending on the structure of the ligand. Intuitively, in the case of the THF-containing complexes the incorporated THF molecules may be assumed to occupy the sixth or the fifth and sixth coordination sites at iron, respectively. However, it seems that incorporation of solvent molecules simply depends on an—as yet not understood—interplay of the mode of preparation with the bulkiness of the side chains at the phenyl rings of the ligand. In the case of the unsubstituted ligand **1,** the isolated complex is solvent-free. From ligands **2** and **4,** which carry rather small alkoxy side chains, complexes with one equivalent of THF are produced, whereas the bulkier substituents in ligands **2**, **5**, and **6** favor the incorporation of two molecules of THF. It seems that THF incorporation is not functionally associated with a possible coordination to the iron center because the solid-state spin-state characteristics (and hence the propensity to catalytically decompose hydrogen peroxide) of the complexes are not affected by the

(73) Zipplies, M. F.; Lee, W. A.; Bruice, T. C. *J. Am. Chem. Soc.* **1986**, *108*, 4433−4445.
(74) Mauerer, B.; Crane, J.; Schuler, J.; Wieghardt, K.; Nuber, B. *Angew. Chem.* **1993**, *105*, 306−308.

presence/absence of additional solvent molecules in the solid state (see Table 2). We propose that the alkoxy side chains affect the packing of the complex molecules so that cavities are formed which allow inclusion of one or two THF molecules, depending on the bulkiness of the side groups. This hypothesis is supported by the fact that extensive exposure of these complexes to high vacuum leads to a partial loss of THF, but it appears impossible to remove the solvent molecules completely. Unfortunately, attempts to produce crystalline material suitable for X-ray analysis in order to prove this hypothesis have failed so far.

The effect of the added nitrogen base, viz. triphenylamine vs trialkylamines, in the preparation procedure is peculiar. We interpret the fact that in one case (**2**) an iron(II) complex can be isolated on mixing the ligand with Fe^{III} chloride and triphenylamine in a way that triphenylamine acts as an one-electron reductant for Fe^{III}, thereby being oxidized to its radical cation. An iron(II) complex now might be formed in which Fe^{II} is weakly bound to the monoanion of the ligand, as deduced from the elemental composition. Due to its low solubility, this complex (**2-Fe^{II}Cl·2THF**) then rapidly precipitates. The desired Fe^{III} complex **2-Fe^{III}Cl·THF** is likely to be formed competitively in a much slower process, which would account for its low yield. However, it cannot be ruled out that the initially produced Fe^{II} ion also gives rise to a second complex in which the Fe^{II} ion indeed occupies the cavity of the now fully deprotonated [N_4] macrocycle. This minor, more soluble fraction of the "correct" Fe^{II} complex might be reoxidized to complex **2-Fe^{III}Cl·THF** by the simultaneously generated triphenylamine radical cation.

As mentioned in the Introduction, the catalytic activity of iron complexes/enzymes depends crucially on the oxidation and spin state of the central iron ion. Natural Fe^{III} porphyrins with octahedral coordination are typically of low-spin ($S = {}^1/_2$) state, whereas axial halide or sulfide ligands in pentacordinated porphyrins favor the high-spin ($S = {}^5/_2$) state. In weakly coordinated or strongly distorted complexes a quantum-mechanically admixed spin state ($S = {}^5/_2, {}^3/_2$) has been reported (see ref 72 for leading references). In the past, a limited number of pentacordinated Fe^{III} complexes of pure intermediate-spin (quartet, $S = {}^3/_2$) state have been described.[75−78] Specifically, Keutel et al.[72] reported on the iron(III)-iodine complex **7-Fe^{III}I** of a 14-membered [N_4] macrocycle that is structurally closely related to our ligands, clearly establishing its pure intermediate-spin state. X-ray structural analysis revealed a square-pyramidal coordination, with the Fe^{III} ion being located 0.34 Å above the plane of the four nitrogen atoms. A similar spin state was expected for our Fe^{III} complexes, at least for the solvent-free preparations. This turned out to be the case for the catalytically active complex preparations (see below), as unequivocally demonstrated by the magnetic susceptibilites (Figures 1, S2−S4) in combination with the Mössbauer spectra (Figures 2, S5− S10). The Mössbauer data of the major component of the Fe^{III} complexes of ligands **1**−**3** (Table 1) are in excellent agreement with the data reported for **7-Fe^{III}I**.[72] The deviations of the effective magnetic moments from the spin-only value of $\mu_{eff} = 3.87\mu_B$ are due to the presence of (primarily) low-spin and high-spin Fe^{III} and/or Fe^{II} impurities, the fraction of which in turn can be assessed from the Mössbauer spectra. Interestingly, the intermediate-spin state is even preserved in the THF-containing preparations. This unexpected observation probably implies that in the solid state the incorporated solvent molecules do not seem to occupy the sixth coordination position at iron or are too weak to change the square-pyramidal coordination toward an octahedral one, for which a $S = {}^1/_2$ state is expected. The Mössbauer data clearly identify **6-Fe^{III}Cl** as an almost pure high-spin ($S = {}^5/_2$) complex.

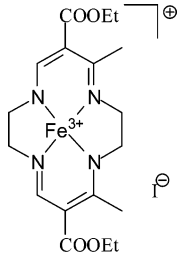

7-Fe^{III}I

The combined spectroscopic properties indicate that the minor high- and low-spin components in our preparations are due to structurally different complexes rather than due to a possible spin-state equilibrium of the same complex. We propose that in all high-spin species the Fe^{III} ion is rather weakly bound to the macrocyclic ligand, probably residing on the surface of the ligand rather than fully occupying the tetraaza cavity. The same is true for the Fe^{II} complex obtained on reaction of **2** with iron(III) chloride in the presence of triphenylamine. There is some reason to assume that in these complexes one or both of the two amine groups of the [N_4] ligand are still protonated because the UV/vis (Figure S1a) and the ESI-MS spectra both exhibit the characteristic features of the bare, iron-free ligand. These observations suggest a ready dissociation of these complexes in solution to give solvent-coordinated iron species and release of the [N_4] ligand in its neutral or anionic form. The latter then would be rapidly protonated by traces of water or by methanol under the conditions of the UV/vis measurements and the ESI-TOF MS measurements, respectively.

Contrary to the straightforward picture obtained from the Mössbauer and susceptibility data, the related EPR spectra of our complexes recorded in frozen DMSO solution at 77 K appear to be rather peculiar. For all preparations which show a catalase-like activity, the EPR spectra are dominated by the characteristic resonances of low-spin iron(III) in the $g = 2$ region (Figure S11 and Table S2), but they are always accompanied by the typical signals of high-spin iron(III) at $g = 5-9$ and ca. 4.2. The relative intensity of the low- and high-spin Fe^{III} signals somehow parallels the yield of oxygen

(75) Kostka, K. L.; Fox, B. G.; Hendrich, M. P.; Collins, T. J.; Rickard, C. E. F.; Wright, L. J.; Münck, E. *J. Am. Chem. Soc.* **1993**, *115*, 6746−6757.
(76) Ikeue, T.; Saitoh, T.; Yamaguchi, T.; Ohgo, Y.; Nakamura, M.; Takahashi, M.; Takeda, M. *Chem. Commun.* **2000**, 1989−1990.
(77) Meyer, K.; Bill, E.; Mienert, B.; Weyhermüller, T.; Wieghardt, K. *J. Am. Chem. Soc.* **1999**, *121*, 4659−4876.
(78) Sakai, T.; Ohgo, Y.; Ikeue, T.; Takahashi, M.; Takeda, M.; Nakamura, M. *J. Am. Chem. Soc.* **2003**, *125*, 1328−1329.

from hydrogen peroxide degradation, i.e., the more intense the high-spin features are, the weaker are the low-spin signals and the lower is the oxygen production (see below). Most remarkably, however, in no case are EPR signals detected which unambiguously can be attributed to the $S = {}^3/_2$ spin state. For the structurally related Fe^{III} complex **7-Fe^{III}I** it has been reported that the intermediate spin state is EPR-silent in the solid state down to 6 K, likely due to magnetic ordering of the iron spins, but an intense, well-defined quartet-state spectrum has been recorded in frozen toluene solution at 10 K.[72] While it is conceivable that similar magnetic interactions in the solid state may cause EPR silence of the intermediate state of our complexes too, this would be quite unusual for a glassy DMSO matrix. Nonetheless, we have to assume that the EPR silence is caused by magnetic interaction phenomena, giving rise to excessive line broadening beyond detection. Thus, in correspondence with the Mössbauer spectra, the detected, rather weak high- and low-spin EPR signals are attributed to residual high- and low-spin iron(III) species from the preparation procedures and/or produced by DMSO coordination.

A few comments are worth reporting concerning the singlet signal at $g \approx 2.001$ observed in the EPR spectra of several preparations of our complexes. The intensity of this isotropic signal, which is observed in the solid state at 77 K (Figure S11) as well as in liquid DMSO solution at room temperature, varies strongly between the various complexes and also for material obtained by the different preparation procedures. The *g*-value and the narrow line width of about 1.5−2 mT (no indication for an additional hyperfine splitting can be found) imply that this resonance is due to an organic radical species. We note that the spectral features of this signal are strikingly similar to that of an oxyl radical center produced at the *meso*-position of an oxygenated Fe^{II} porphyrin complex reported recently.[79] Double integration of the EPR spectra and the satisfying elemental analyses confirm that this signal represents only a minor (≤2%) byproduct. We tentatively attribute this signal to a phenoxyl-type radical,[80] which would be in line with the two weak electronic absorptions at about 515 and 545 nm observed only in the UV/vis spectra of those samples for which this EPR signal is rather strong.

All complexes are subjected to the reaction with hydrogen peroxide in order to test their ability to act as catalase mimic. As shown in our preliminary communication,[52] **2-Fe^{III}BF$_4$** proved to be an efficient catalase mimic, decomposing hydrogen peroxide under physiological conditions to oxygen and water in high yield according to the catalase stoichiometry. The data of Table 2 reveal a similar reactivity for the other complex preparations of major intermediate spin in the solid state. The varying composition of the preparations, however, impedes any conclusion concerning the dependence of the catalytic efficiency on the substitution pattern.

Complex **6-Fe^{III}Cl**, which, independent of the preparation procedure, could only be isolated as a high-spin species, is the only totally inactive complex with regard to oxygen release from H_2O_2. In fact, hydrogen peroxide is decomposed by this complex only in a stoichiometric fashion, i.e., H_2O_2 decomposition amounts to about 5% at our standard conditions (5 μM complex, 100 μM H_2O_2). In agreement, the Fe^{III} complex of the tetramethyl-substituted derivative of ligand **1**, which had been prepared earlier and shown to be a pure high-spin Fe^{III} complex,[81] did not release oxygen when exposed to hydrogen peroxide.[82] These observations clearly indicate that the spin state of the iron center is crucial for the capability of the complexes to act as a catalase mimic, i.e., to produce oxygen and water. Since the high-spin complexes of our ligands are catalytically inactive, we assume that in these complexes the high-spin state is conserved in aqueous solution. In which spin state the iron center of the catalytically active complexes exists in aqueous solution remains unclear so far; however, one would expect that in aqueous (buffered) solution the pentacoordinate Fe^{III} intermediate-spin complexes are converted to hexacoordinate low-spin species in which the axial sites are occupied by water and/or hydroxyl anions, rather than preserving the intermediate-spin state of the solid material. Unfortunately, the solubility of the complexes in water is too low to prove this hypothesis by EPR spectroscopy or magnetic measurements. However, quantum-chemical density functional theory (DFT) calculations which were recently published[60] predict that H_2O_2 decomposition in terms of a catalase-like mechanism may proceed on the doublet- as well as on the quartet-state hypersurface with virtually identical energies.

For four preparations, turnover numbers, i.e., the moles of hydrogen peroxide decomposed per mole of catalyst, are determined (Table 2). The turnover numbers, which are a better measure of the catalase-like activity than the relative oxygen yields, reveal that the catalysts are deactivated after 40 to 80 catalytic cycles. The linear dependence of the initial rate of oxygen release on the concentration of the catalysts and H_2O_2, respectively (Figure 4), indicates that the first step of the catalytic cycle—reaction of the iron(III) complex with H_2O_2—is rate-determining. The second-order rate constants show only a minor variation, within a factor of 2 (ca. 1200−2400 M^{-1} s^{-1}), with the structure of the macrocyclic ligand. These rate constants are 2500−5000 times lower than values typically found for native catalase ($k_{cat} = 6 \times 10^6$ M^{-1} s^{-1}).[83]

From the data of Table 2 and Figure 4 it is evident that under our standard reaction conditions the yields of oxygen barely exceed 87% of the theoretical amount, although all of the H_2O_2 has finally been decomposed. Thus, there must be at least a second route of degradation by which 10−20% of the H_2O_2 is decomposed without release of molecular

(79) Balch, A. L.; Noll, B. C.; Olmstead, M. M.; Phillips, S. L. *Inorg. Chem.* **1996**, *35*, 6495−6506.

(80) Since this radical is not observed in preparations of the unsubstituted complex **1-Fe^{III}X** (see, e.g., Figure S11a), formation of a phenoxyl-type radical can reasonably be explained by one-electron oxidation of the alkoxyl-substituted macrocyclic ligand to its radical cation, followed by rapid O−C scission of the side chain by carbenium ion elimination.

(81) Goedken, V. L.; Molin-Case, J.; Whang, Y.-A. *J. Chem. Soc., Chem. Commun.* **1973**, 337−338.

(82) Baute, J. Doctoral thesis, Universität Duisburg-Essen, 2003.

(83) *Methods of Enzymatic Analysis*, 3rd ed.; Bergmeyer, J., Grassl, M., Eds.; Verlag Chemie: Weinheim, Germany, 1983; Vol. II, p 165.

Scheme 4. Proposed Catalytic Cycle for Decomposition of Hydrogen Peroxide by 1,4,8,11-Tetraaza[14]annulene Fe^{III} Complexes

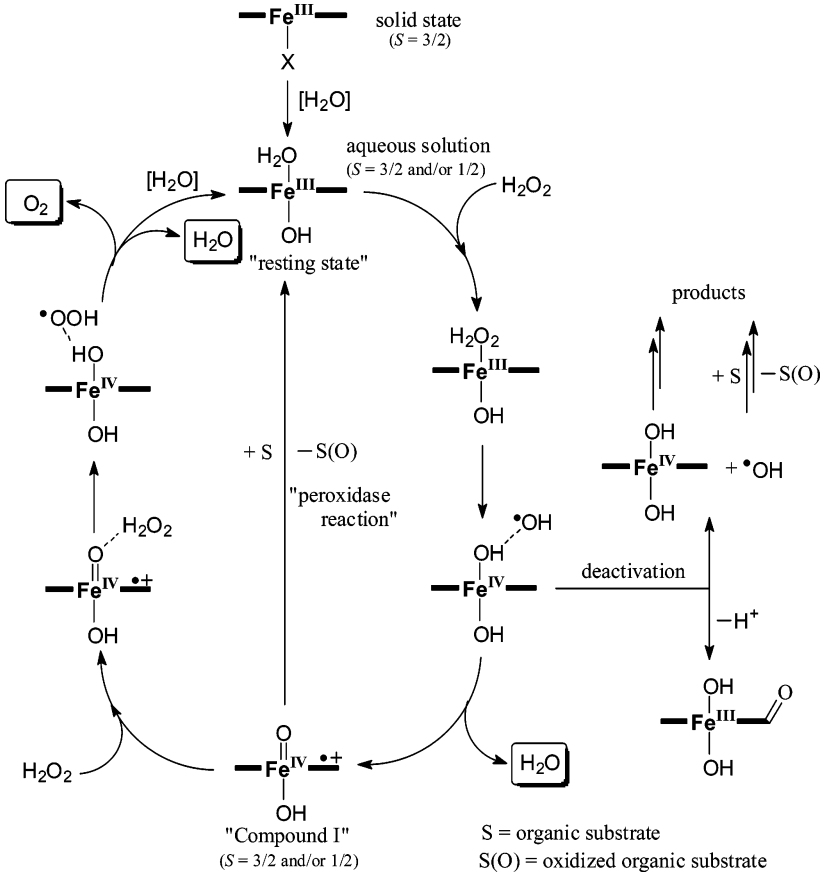

oxygen. As our complexes are modeled according to the coordination pattern of the heme system of catalases and peroxidases it is reasonable to assume a similar mechanism of hydrogen peroxide decomposition as discussed for these enzymes. In the catalytic cycles of these heme complexes, an oxoferryl species ligated by the π-radical cation of the porphyrin ligand (por$^{\bullet+}$Fe^{IV}=O), the so-called Compound I, is a pivotal intermediate.[2,11−13] In the above-mentioned DFT study on the reaction of the parent iron(III) complex **1-Fe^{III}OH** with hydrogen peroxide, it is found that a Compound I-like species is an intermediate in our system too.[60] In line with the above kinetic data, the computations predict that formation of this species by reaction of the Fe^{III} complex ("resting state") with the first molecule of hydrogen peroxide is the rate-limiting step. With regard to the known reactivity of ferryl-oxo (Fe^{IV}=O) species, it can be expected that this Compound I analogue is involved in both the catalase-like conversion of hydrogen peroxide as well as the oxygenation reactions exercised by peroxidases. Both classes of enzymes possess the same active heme center, and substrate specifity is achieved by the surrounding protein. Catalase offers access to the active center only to small molecules like hydrogen peroxide through a small channel; peroxidase provides a more open access to the heme group and thus can be approached by bigger molecules with concomitant one-electron oxidation of the substrates. Our present catalysts, however, are lacking the substrate-directing function of a protein environment. Therefore, the competing peroxidase pathways of the catalysts will become more important when the H_2O_2 concentration decreases in the course of reaction because in the second step of the catalase cycle Compound I is reduced by a second molecule of hydrogen peroxide with release of oxygen. This is clearly indicated by the time profiles displayed in Figure 5, which confirms that at the early stage of the reaction the oxygen production is indeed quantitative with respect to the 2:1 stoichiometry of catalase. With reference to the computational studies,[60] the present observations are rationalized by the catalytic cycle displayed in Scheme 4.

The most likely substrate in our reaction mixtures for the peroxidase-like process is DMSO. Because of the low water solubility of our complexes, the reaction mixtures are made up by adding aliquots of a 5 mM DMSO stock solution of the catalysts to the aqueous buffer to give the desired final concentration of 5 μM. Then the appropriate amount of hydrogen peroxide is added. Hence, DMSO is in great excess (ca. 22 mM) to the catalyst. ^{13}C and ^{1}H NMR experiments in which 6 mM H_2O_2 was decomposed by 0.4 mM **2-Fe^{III}BF$_4$** in the presence of 2.6 mM DMSO indeed support the presumption that DMSO is a substrate of the reactive intermediate(s).[52] Dimethyl sulfone, which is commonly regarded as a two-electron oxidation product, was detected as the main product.[82] This product is likely to result from oxygen transfer from the putative Compound I analogue to DMSO.[84] Our computations also indicate that the formation of the oxoferryl species proceeds via O−O bond homolysis of the Fe^{III}-ligating hydrogen peroxide,[60] whereby free hydroxyl radicals may be released. In line with the theoretical

prediction, the intermediacy of HO• radicals is clearly indicated by the detection of minor amounts of [D_3]-methanesulfonic acid, [D_3]methanol, and [D]formate,[82] products which are characteristic for attack of HO• on DMSO.[85]

The formation of hydroxyl radicals might also be a major reason for deactivation of the catalysts. The DFT computations also reveal that during the mentioned homolytic O−O bond breaking process the generated HO• radical is in a perfect structural arrangement for undergoing addition to the *meso*-carbon (the central carbon of the diaza-propylidene unit) of the macrocyclic ligand.[60] This hydroxylation reaction finally may lead to oxidative degradation of the tetraaza macrocycle, similar to what is known for the oxidative degradation of heme porphyrins.[86] Further experiments to elucidate the deactivation processes of the catalysts will be carried out. In addition, the formation of dimethylsulfone suggests that these catalysts might also be active in transferring oxygen to other compounds than DMSO, for instance transfer of oxygen to C−C double bonds yielding oxiranes or 1,2-diols, as is known for many compounds of this type.[87] Experiments in this direction are under way.

Acknowledgment. This work was supported by the Deutsche Forschungsgemeinschaft (SFB 452).

Supporting Information Available: Preparative procedures for the ligand precursors and Fe^{III} complexes, two figures of UV/vis spectra and a table of absorption maxima of the ligands and iron complexes, six figures of temperature-dependent molar susceptibilities, seven figures of Mössbauer spectra and related explanations, a figure of EPR spectra and a table of related *g*-values, a figure of the H_2O_2 dependence of oxygen yields, and two figures of the catalyst dependence of oxygen yields. This material is avaible free of charge via the Internet at http://pubs.acs.org.

IC700961B

(84) In preliminary stopped-flow experiments no clear evidence for formation of a Compound-I-like species could be found in the ms time range (unpublished results). This would be in agreement with the high reactivity of such a species and the fact that its formation is rate-determining.

(85) Lehnig, M.; Kirsch, M.; Korth, H.-G. *Inorg. Chem.* **2003**, *42*, 4275−4287.

(86) Ortiz de Montellano, P. R. *Acc. Chem. Res.* **1998**, *31*, 543−549.

(87) Kumar, D.; de Visser, S. P.; Shaik, S. *J. Am. Chem. Soc.* **2003**, *125*, 13024−13025.